

**THE EFFECTS OF LASER SURFACE TEXTURING ON
LUBE OIL CONSUMPTION OF A HEAVY DUTY DIESEL
ENGINE**

**M.Sc. Thesis by
Ahu TOYGAR, B.Sc.**

**Department : Mechanical Engineering
Programme : Automotive**

Supervisor : Assist. Prof. Dr. Özgen AKALIN

JUNE 2008

**THE EFFECTS OF LASER SURFACE TEXTURING ON
LUBE OIL CONSUMPTION OF A HEAVY DUTY DIESEL
ENGINE**

**M.Sc. Thesis by
Ahu TOYGAR, B.Sc.**

**Date of submission : 5 May 2008
Date of defence examination: 11 June 2008**

**Supervisor (Chairman): Assist. Prof. Dr. Özgen AKALIN
Members of the Examining Committee Prof.Dr. Metin ERGENEMAN (İTÜ)
Prof.Dr. Mustafa ÜRGEN (İTÜ)**

**LAZER İLE YÜZEY İŞLEMENİN BİR AĞIR HİZMET
DİZEL MOTORUNUN YAĞ TÜKETİMİNE
ETKİLERİ**

**YÜKSEK LİSANS TEZİ
Ahu TOYGAR
(503051716)**

**Tezin Enstitüye Verildiği Tarih : 5 Mayıs 2008
Tezin Savunulduğu Tarih : 11 Haziran 2008**

**Tez Danışmanı : Yrd. Doç. Dr. Özgen AKALIN
Diğer Jüri Üyeleri Prof.Dr. Metin ERGENEMAN (İTÜ)
Prof.Dr. Mustafa ÜRGEN (İTÜ)**

ACKNOWLEDGEMENT

First of all I would like to thank to my thesis advisor Dr. Özgen Akalın who has given me the chance to complete this Master of Science thesis, for his invaluable guidance, advice and encouragement throughout this work.

This study was a part of the project “Power Cylinder Design for Optimized Lube Oil Consumption” which is sponsored by Ford Otosan A.Ş and I would like to thank the company for their financial and technical support. I am also grateful to Ö. Rüştü Ergen, Nedim Güngör Soydemir and Göktan Kurnaz for their cooperation in this project.

I also would like to thank Emrah Özgümüş and OTAM (Automotive Technology Research and Development Center) staff for their invaluable support and friendly attitude during oil consumption measurement tests.

I also would like to express my gratitude to Prof. Dr. Metin Ergeneman and Dr. Akın Kutlar for their priceless advice and also my project partners Selçuk Çobanoğlu and O. Taha Şen for their assistance and support in this work.

Lastly, I am also grateful to my family for their everlasting guidance and inspiration.

May, 2008

Ahu TOYGAR

TABLE OF CONTENTS

ABBREVIATION	vi
LIST OF TABLES	vii
LIST OF FIGURES	viii
LIST OF SYMBOLS	x
SUMMARY	xi
ÖZET	xii
1. INTRODUCTION	1
1.1 Fundamentals of Tribology	3
1.1.1 Wear	4
1.1.2 Lubrication Regimes	6
1.1.2.1 Hydrodynamic Lubrication	6
1.1.2.2 Elastohydrodynamic Lubrication	6
1.1.2.3 Mixed Lubrication.....	7
1.1.2.4 Boundary Lubrication.....	8
1.1.3 Surface Texture Parameters.....	9
1.2 Laser Structuring	11
1.2.1 Laser Structuring of Cylinder Working Surfaces.....	12
1.2.2 Machining the Cylinder Working Surfaces.....	13
1.2.3 Laser Structuring of Other Functional Surfaces.....	16
1.3 Oil Transport Mechanisms of IC Engines.....	17
1.3.1 Piston-Ring Pack	17
1.3.1.1 Oil Transport through the Ring Grooves.....	18
1.3.1.2 Oil Transport from the Piston Land into the Grooves.....	18
1.3.1.3 Oil Transport from the Grooves to the Lands	20
1.3.1.4 Oil Flow through the Ring Gaps	21
1.3.2 Turbocharger	21
1.3.3 Valve Guide Leakage	22
1.4 Oil Consumption Measurement Methods for Internal Combustion Engines	23
1.4.1 Conventional Oil Consumption Measurement Methods.....	24

1.4.2 Tracer Methods.....	31
1.4.3 Analytical Prediction Studies.....	33
1.5 Literature Survey.....	34
1.5.1 Experimental Studies on Laser Surface Texturing.....	34
1.5.2 Theoretical Studies on Laser Surface Texturing.....	40
1.6 Objective.....	43
2. EXPERIMENTAL METHOD.....	44
2.1 Instrumentation of Measurement System and Test Requirements.....	44
2.1.1 Experimental Setup.....	44
2.1.2 Test Lubricating Oil.....	47
2.1.3 Test Fuel.....	48
2.1.4 Mass Spectrometer.....	48
2.1.4.1 The V&F Twin MS Technology and Instrumentation.....	49
2.1.5 Oxidation Furnace.....	53
2.1.6 Heated Line.....	54
2.1.7 Test Engine Specification.....	54
2.2 Determination of Oil Consumption Based on Mass Spectrometry.....	57
2.2.1 Test Procedure.....	57
2.2.2 Calculation of Oil Consumption.....	58
2.2.3 Calculation of Exhaust Molar Mass.....	61
2.2.4 Test Matrix.....	62
3. EXPERIMENTAL RESULTS.....	64
3.1 Lube Oil Consumption Results.....	64
3.2 Specific Oil Consumption Results.....	71
4. CONCLUSION AND FUTURE RECOMMENDATIONS.....	77
REFERENCES.....	79
APPENDICES.....	84
CURRICULUM VITAE.....	89

ABBREVIATIONS

S	: Sulfur
SO₂	: Sulfur dioxide
LST	: Laser Surface Texturing
PM	: Particulate Matter
HC	: Hydrocarbon
IC	: Internal combustion
T	: Tritium
Br	: Bromine
ppm	: Particulate per million
LIF	: Laser Induced Fluorescence
C	: Carbon
Mg	: Magnesium
Ge	: Germanium
Ca	: Calcium
CO₂	: Carbon dioxide
Xe	: Xenon
Kr	: Krypton
Hg	: Mercury
N₂	: Nitrogen gas
CO	: Carbon monoxide
H₂SO₄	: Sulfuric acid
g/h	: Gram per hour
kg/h	: Kilogram per hour
MS	: Mass spectrometer
amu	: Atomic mass unit
IMR	: Ion Molecule Reaction
m/z	: Mass to charge ratio
DI	: Direct Injection
EHL	: Elaso-hydrodynamic lubrication
SiC	: Silicon carbide
Nd:YAG	: Neodymium-doped yttrium aluminium garnet
PID	: Proportional-integral-derivative
P_{me}	: Mean effective pressure
rpm	: Revolutions per minute

LIST OF TABLES

	Page No.
Table 2.1 : Technical Specification and Rating Data of V&F Twin MS.....	53
Table 2.2 : Test Engine Specifications.....	54
Table 2.3 : Test Matrix.....	63
Table 3.1 : Lube Oil Consumption Results.....	64
Table 3.2 : Cylinder Surface Texture Parameters for Engine.....	70
Table 3.3 : Specific Oil Consumption Results.....	71
Table C.1 : Measurement and Oil Consumption Results of Test Engine (Cylinders 1-3).....	87
Table D.1 : Measurement and Oil Consumption Results of Test Engine (Cylinders 4-6).....	88

LIST OF FIGURES

	Page No.
Figure 1.1 : Losses in the Combustion Engine.....	2
Figure 1.2 : Build-up of Hydrodynamic Pressure.....	4
Figure 1.3 : Rubbing of Two Contact Surface.....	5
Figure 1.4 : Stribeck Curve.....	8
Figure 1.5 : Schematic of Bearing Ratio Plot.....	11
Figure 1.6 : Different Dimple Shapes.....	14
Figure 1.7 : Beam Guiding in a Laser Machining Plant and in a Laser Head System.....	15
Figure 1.8 : Process Sequence of Laser Structuring of Cylinder Working Surfaces.....	15
Figure 1.9 : Description of Oil Transport into the Ring Groove.....	19
Figure 1.10 : Effect of Ring Static Twist on the Rate of Oil Squeezing.....	21
Figure 1.11 : Oil Blow through End Gap into the Combustion Chamber.....	22
Figure 1.12 : Turbocharger Bearing System.....	22
Figure 1.13 : Schematic of Valve Guide Leakage.....	23
Figure 1.14 : Classification of Oil Consumption Measurement Methods.....	25
Figure 1.15 : Schematic of Oil Pump System.....	27
Figure 1.17 : Oil Level Change Rate Device.....	29
Figure 1.16 : Gravity Fed Measurement System.....	28
Figure 1.17 : Smart Oil Consumption Measurement.....	29
Figure 1.18 : AVL 406 Oil Consumption Meter.....	30
Figure 2.1 : Schematic of Exhaust Gas Sampling System.....	45
Figure 2.2 : Schematic of Sample Probe Mounting.....	46
Figure 2.3 : Basic Components of Mass Spectrometer.....	49
Figure 2.4 : V&F Twin MS.....	50
Figure 2.5 : Quadrupole Mass Filter.....	51
Figure 2.6 : Schematic Structure of V&F Twin MS.....	52
Figure 2.7 : Configuration of Cylinder Blocks.....	56
Figure 2.8 : Calculation Flowchart.....	58
Figure 3.1 : Oil Consumption at 25% Load.....	65
Figure 3.2 : Oil Consumption at 50% Load.....	66
Figure 3.3 : Oil Consumption at 75% Load.....	67
Figure 3.4 : Oil Consumption at 100% Load.....	67
Figure 3.5 : Oil Consumption at 1000 rpm.....	68

Figure 3.6	: Oil Consumption at 1600 rpm.....	69
Figure 3.7	: Oil Consumption at 2200 rpm.....	70
Figure 3.8	: Specific Oil Consumption at 1000 rpm.....	72
Figure 3.9	: Specific Oil Consumption at 1600 rpm.....	72
Figure 3.10	: Specific Oil Consumption at 2200 rpm.....	73
Figure 3.11	: Specific Oil Consumption at 25% Load.....	74
Figure 3.12	: Specific Oil Consumption at 50% Load.....	74
Figure 3.13	: Specific Oil Consumption at 75% Load.....	75
Figure 3.14	: Specific Oil Consumption at 100% Load.....	76

LIST OF SYMBOLS

\dot{m}_E	: Exhaust mass flow
\dot{m}_A	: Intake air mass flow
\dot{m}_F	: Fuel mass flow
\dot{n}_E	: Mol flow of exhaust
$\dot{m}_{SO_2,E}$: SO ₂ mass flow in the exhaust
$\dot{m}_{S,F}$: S mass flow contribution of fuel
$\dot{m}_{SO_2,F}$: SO ₂ mass flow contribution of fuel
$\dot{m}_{SO_2,O}$: SO ₂ mass flow contribution of oil
$\dot{m}_{S,O}$: S mass flow contribution of oil
\dot{m}_O	: Oil mass flow
\dot{m}_{OC}	: Oil consumption rate
N	: Total mol number of exhaust
S_{oil}	: S concentration in oil
S_{fuel}	: S concentration in fuel
M_E	: Molar mass of exhaust

THE EFFECTS OF LASER SURFACE TEXTURING ON LUBE OIL CONSUMPTION OF A HEAVY DUTY DIESEL ENGINE

SUMMARY

This study aims to accomplish the development of a real time sulfur tracing method employing a quadrupole mass spectrometer. The analysis of sulfur dioxide concentration in the exhaust stream which provides determination the amount of lube oil consumption in two different cylinder groups having dissimilar honing pattern is the major task of the study. For this purpose, a turbo-charged heavy-duty diesel engine with six cylinders having first three cylinders (Cylinder 1-3) standard plateau honing pattern and last three cylinders (Cylinders 4-6) laser honing pattern is utilized.

Since controlling lube oil consumption of internal combustion engines is becoming more important due to stringent emission regulations, engine functionality and customer satisfaction, accurate and fast measurement of oil consumption gets high priority. In this study sulfur tracer method is preferred due to its advantages such as possibility of real time oil consumption, capability of measuring oil consumption of each cylinder group and enabling fast and accurate results. Moreover, high sulfur content lubricant oil and low sulfur content fuel are required for the experiments based on sulfur tracer method.

A sampling system is designed to measure the oil consumption of separate cylinder groups sequentially under identical operating conditions. The developed method enables the comparison of oil consumption of each cylinder group at each point of test matrix without changing engine operating conditions. The effects of laser surface texturing on lube oil consumption of the test engine are investigated and the experimental results are presented by means of comparative graphs based on the effects of engine power and revolution. Furthermore a discussion is done about laser surface texturing effects on lube oil consumption in order to determine the most effective surface texture parameters for utilization of laser structuring.

LAZER İLE YÜZEY İŞLEMENİN BİR AĞIR HİZMET DİZEL MOTORUNUN YAĞ TÜKETİMİNE OLAN ETKİLERİ

ÖZET

Bu çalışma, özel bir ağır hizmet dizel motorunun yağ tüketiminin, gerçek zamanlı sülfür izleme yöntemi kullanılarak kütle spektrometresi aracılığıyla ölçümünü hedeflemektedir. Çalışmadaki başlıca yöntem, farklı honlama özelliğine sahip üçlü silindir gruplarına ait egzoz gazı sülfür dioksit konsantrasyonlarını analiz ederek yağ tüketim miktarlarını belirlemektir. Bu amaçla, üç silindiri (Silindirler 1-3) plato honlanmış ve diğer üç silindiri (Silindirler 4-6) lazerli honlanmış olan aşırı doldurmalı ve altı silindirli bir ağır hizmet dizel motoru kullanılmıştır.

Yağ tüketiminin kontrolü gittikçe sertleşen emisyon regülasyonları, motor işlevselliği ve müşteri memnuniyeti gibi faktörler açısından daha da önemli hale gelmekte olduğundan, yağ tüketiminin doğru ve hızlı ölçümü büyük öncelik taşımaktadır. Bu çalışmada, ölçüm yöntemi olarak, gerçek zamanlı yağ tüketimi ölçümü, farklı silindir gruplarının ayrı ayrı yağ tüketimi ölçümü ve hızlı ve doğru sonuçlar sağlığı gibi avantajları doğrultusunda sülfür izleme yöntemi ölçüm yöntemi olarak tercih edilmiştir. Sülfür izleme yöntemine dayanan bu deneylerde yüksek sülfür içeren yağlama yağı ve düşük sülfür içeren yakıt kullanılmıştır.

Her iki silindir grubu için de aynı motor çalışma koşullarını sağlamak üzere, özel bir örnek toplama sistemi tasarlanmıştır. Geliştirilen bu yöntem, motor çalışma koşullarını değiştirmeden her iki silindir grubundan ardışık olarak örnek alınmasına ve böylece yağ tüketim miktarlarının test matrisine ait her bir çalışma noktası için karşılaştırılmasına imkan vermektedir. Lazerli yüzey işlemenin test motorunun yağ tüketimi üzerindeki etkileri araştırılmış ve deneysel sonuçlar, karşılaştırmalı grafiklerle motor güç ve devir sayısına bağlı olarak sunulmuştur. Ayrıca, lazerli honlama işleminden daha çok yararlanmak amacıyla en etkili yüzey işleme parametreleri belirlenerek lazerli yüzey işlemenin yağ tüketimi üzerine etkileri yorumlanmıştır.

1. INTRODUCTION

Reduction of friction and the amount of wear on machine element components involved in sliding contact is always desired. The efficiency, reliability and durability of such components depend on the friction that occurs at the sliding contact interface. Since more energy saving engines becomes more preferable in today's world, the load capacity or the power density of these machine elements is the major aim, which of course will lead to higher severity of surface interaction.

Another factor that motivates engine research is the environmental pollution. Stricter emission regulations have been enforced on automobiles in order to preserve air quality, because they are considered to be a major contributor to pollution, thus the automotive industry has been searching for possible solutions.

It is obvious that, the criteria for designing engine should include fulfilling of high energy efficiency and low emission level. Since, energy efficiency and emissions are determined by factors such as friction level and lubrication system of the engine, piston-ring-liner system becomes the main contributor to the engine friction and emission. In Figure 1.1, the losses in the combustion engine are illustrated. Both of these needs mentioned above, require effective lubrication strategy for sliding surfaces. When the fuel (chemical energy) is ignited in the combustion chamber, the explosive force from the burning fuel pushes the piston into a reciprocating motion (kinetic energy). The highly dynamic forces, during the reciprocating motion in the cylinder, often result in the wearing of the contact surfaces due to friction. The contacting surfaces include the surfaces between the piston and the piston rings, piston and cylinder bore, piston rings and cylinder bore.

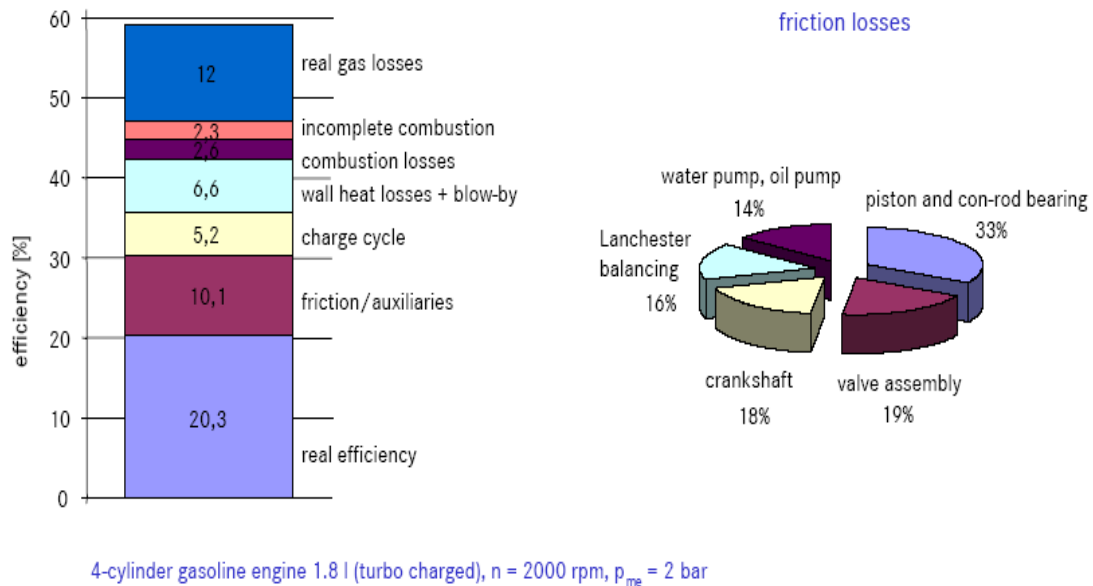


Figure 1.1 Losses in the Combustion Engine

Surface lubrication involves many aspects of the physical and chemical properties of the surface material and the lubricant. The viscosity of the lubricant and some of its other properties determine the thickness of the lubricant fluid film. A thicker lubricant fluid film leads to better lubrication. Similarly, the roughness of the contacting surfaces has a major impact on the friction and wear behavior of lubricated surfaces. In general, smoother surfaces are better for fluid film lubrication.

In recent years, it has been shown that the presence of artificially created micro structures can significantly affect friction and wear behavior of lubricated surfaces. Undulated surfaces created by machining of periodic grooves on the surface of a titanium alloy disc were shown to reduce friction in lubricated reciprocating contact when compared to non-undulated surfaces. The friction reduction was attributed to the trapping of wear debris in the groove. With this recognition, a method has been recently developed to texture seal surfaces with a laser. The process, known as laser surface texturing (LST), involves creation of an array of micro dimples on the seal surface by a material ablation process with a pulsating laser beam. LST produces a very large number of micro-dimples on the surface and each of these micro-dimples can serve either as a micro-hydrodynamic bearing in cases of full or mixed lubrication, a micro-reservoir for

lubricant in cases of starved lubrication conditions, or a micro-trap for wear debris in either lubricated or dry sliding. Thus the oil consumption and the emission of combustion engines can be reduced. The reduction of the friction loss reduces wear which increases the service life of the engines. Apart from applying laser structuring techniques to piston working surfaces, the structuring process is also used on tribological function surfaces on bearings of moveable components and forming tools. In these cases the aim is also to minimize the friction and thus the wear, increasing the service life or durability, respectively.

In this thesis, a real time sulfur measurement method was developed employing a quadrupole mass spectrometer to analyze the sulfur dioxide concentration in the exhaust gas of a heavy duty diesel engine. In order to determine the effects of cylinder bore surface texture parameters on total lube oil consumption of the test engine were investigated simultaneously using a cylinder block having dissimilar honing patterns on each cylinder group. By means of the modification of the test engine, the effects of laser surface texturing of cylinder bores on lube oil consumption was investigated and the comparison of standard plateau honing and laser honing patterns was provided.

1.1 Fundamentals of Tribology

A tribological system consists of the elements of basic solid, counter body and intermediate as well as their properties and interactions as it is shown in Figure 1.2. The lubricant constitutes the intermediate in surfaces sliding on each other. The major task of the lubricant is the reduction of the friction forces between the tribological partners. The properties of the lubricant such as adhesive power, viscosity and resistance to pressure influence the function, as well as collective stress factors of the system such as forces, movements, temperature and time in operation. The lubricant can be utilized completely when the entire surface is wetted uniformly.

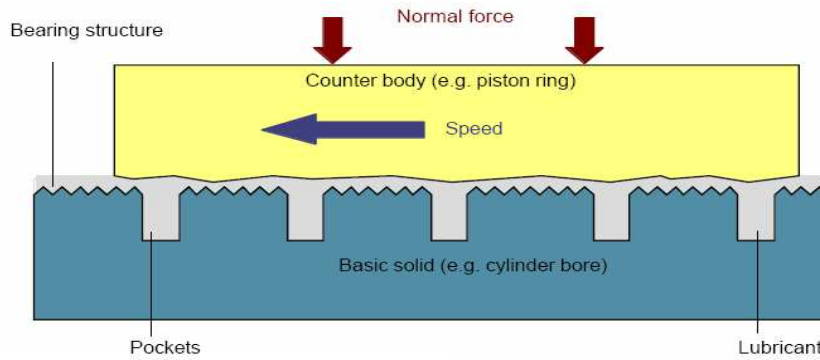


Figure 1.2 Build-up of Hydrodynamic Pressure (Gehring Technical Brochure, 2002)

1.1.1 Wear

The progressive loss of substance from the operating surface or body occurring as a result of relative motion at the surface is defined as wear (Bhushan, 1999). It is incontestable that wear mechanisms are far more complex than this definition. Several wear mechanisms may be operative simultaneously but generally one may play a major role in the control of wear rate. By means of the nature of the contacting surfaces and the type of relative motion occurring at these surfaces, the rate of controlling mechanism can be determined for that surface.

Since extreme mechanical stresses take place in the cylinder, which are caused by high kinetic energy, momentum from piston dynamics, high temperature, pressure during combustion and distortion of metal, wear became a significant problem. Thus, the criteria of efficiency and durability must be achieved by the designs of piston ring packs despite of the severe conditions.

In Figure 1.3, wear of the reciprocating motion of the piston and piston rings against the cylinder liner is shown. Since there occurs a lack of lubricant, piston-ring wear takes place only in boundary and mixed lubrication regimes.

Corrosion, adhesion and abrasion are three major effects which cause wear. In the case of acidic substances in the piston-ring-liner system attacking metal surfaces may cause corrosion. This problem may be eliminated by chemical detergent oils that neutralize the corrosive acids and with proper control of the engine.

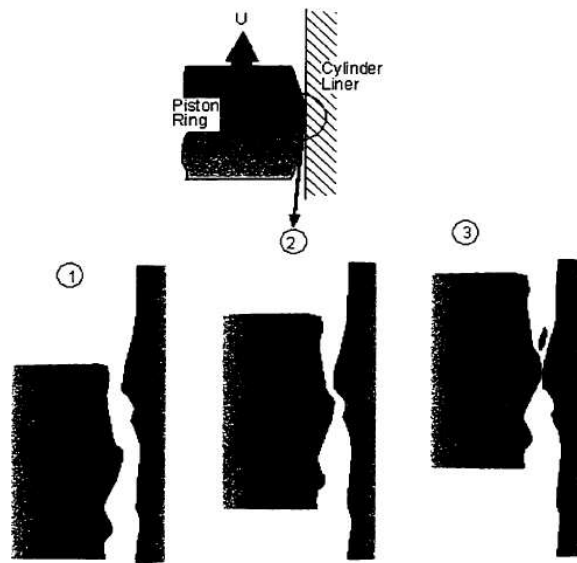


Figure 1.3 Rubbing of Two Contact Surface under Microscopic View

Adhesive Wear: Sliding of two surfaces against each other can cause adhesive wear. High local pressure between contacting asperities results in plastic deformation and formation of local junctions. Breaking of these junctions is consisted by means of relative tangential motion of the surfaces and material is removed or transferred from the softer surface to the harder one. The physical and chemical properties of the materials in contact influence the efficiency to form an adhesive junction. (K. H. Zum Gahr, 1987)

Adhesive wear mainly affects parts of the engine where there is metal-to-metal contact. It becomes significant especially when the engine is at the beginning of operation and is cold due to insufficient oil amount in the cylinder kit assembly.

Abrasive Wear: This type of wear occurs when there are impurities present in the lubricating oil at the contact surfaces. Atmospheric dust and the metallic debris from corrosive and adhesive wear can cause these impurities. The ratio of asperity contact increases when the impurities stay between two contact surfaces, such as piston ring and cylinder liner. Using air filtration, periodic oil changes and filtration of the oil system may eliminate abrasive wear.

1.1.2 Lubrication Regimes

1.1.2.1 Hydrodynamic Lubrication

Hydrodynamic lubrication regime, which is also called fluid film lubrication regime, occurs when the wearing surfaces are completely separated by a film of oil. The friction occurring in an optimized tribological system should consist of hydrodynamic friction only in continuous operating conditions. This condition is also referred to as hydrodynamic lubrication. The condition of hydrodynamic lubrication is achieved when a narrowing gap, relative tangential movement of the sliding surface and a sufficient amount of lubricant are present. In this condition, the thickness of the lubricant film should be distinctly larger than the roughness of the sliding surfaces. In this respect lubricant parameters, such as viscosity and additives, as well as the structure of the functional surfaces render a significant contribution. If the condition of hydrodynamic lubrication no longer exists, then wear mechanisms, such as adhesion and abrasion, will occur.

In this type of regime, liquid film completely separates the basic solid from the counter body and takes the entire stress. Moreover, fluid friction is substituted for mechanical friction in order to reduce friction between moving surfaces (Gehring GmbH & Co. KG Technical Brochure, 2002).

Film thickness: Film thickness can be determined by means of simplified equations in order to provide approximations with a substantial degree of precision. Film thickness can be defined as a function of viscosity, velocity and load. The film thickness increases with viscosity or velocity. When these two variables decrease, the film thickness also decreases. Viscosity and velocity are also affected by oil temperature. Oil velocity is increased by the increase of the operating temperature thus viscosity is reduced. Velocity increases may also cause temperature increases which subsequently result in viscosity reduction.

1.1.2.2 Elastohydrodynamic Lubrication

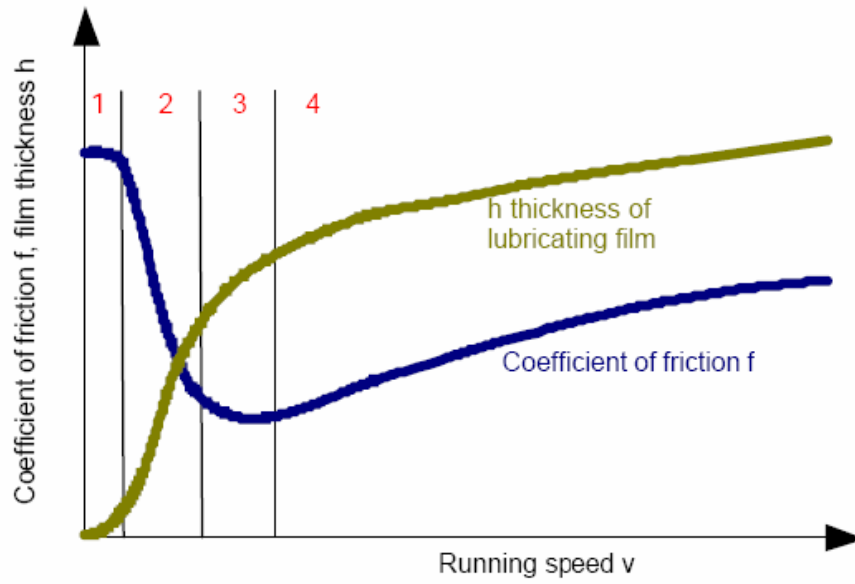
Lubrication principles of rolling objects such as ball or roller bearings, is defined as elastohydrodynamic (EHD) lubrication. There occurs an oil wedge at the lower edge of

the rolling body which is similar to that in hydrodynamic lubrication. A film between sliding element and the supporting surface is initiated with an increase of pressure by means of oil adhesion. Since the contact area is particularly small such as in roller and ball bearing, the force per unit area or load pressure is extremely high. The oil would be completely pressed from between the wearing surfaces in such high pressure cases. On the other hand, high pressure prevents oil from squeezing out causing an increase in viscosity. Therefore a thin film of oil occurs (Harris, 1991)

1.1.2.3 Mixed Lubrication

The lubricant film may be permeated when the pressures in elastohydrodynamically lubricated machine elements are too high or the running speeds are too low. Some contact between asperities subsequently results in mixed lubrication. In other words, if no hydrodynamic lubrication exists, a mixed friction condition is present. In this case the basic solid and the counter body have some contact in roughness peaks. The boundaries between these individual conditions are fluid and can be illustrated by means of the so-called Stribeck curve. The change of friction coefficient f relative to the sliding speed V is showed in the curve which is presented in Figure 1.4. The space between the two friction partners is represented with thickness of the lubricant film h , and has a direct relationship with friction conditions.

Boundary and hydrodynamic lubrication principles are considerably effective for the behaviour of junction in a mixed regime. One or more molecular layers of boundary lubricating films cause interactions. A mixed fluid film lubrication action develops in the volume between the solids.



- | | |
|-------------------------------------|---|
| 1 Boundary friction $\rightarrow 0$ | 3 Elasto-hydrodynamic lubrication ($h > R$) |
| 2 Mixed friction $h \approx R$ | 4 Hydrodynamic lubrication ($h \gg R$) |

Figure 1.4 Stribeck Curve

Mixed lubrication allows much smaller film thicknesses than pure hydrodynamic lubrication or elastohydrodynamic lubrication. Reduced film thickness coincides with increased load and contact pressure, if other factors remain unchanged, and this characteristic is the basic reason for the importance of mixed lubrication.

Although in most cases when this lubrication regime is active the collisions between asperities are prevented from inducing any severe forms of wear, a sudden and severe mode of lubrication failure known as scuffing can occur. This can cause serious industrial problems since scuffing can occur precipitately in an apparently well lubricated contact (Stachowiak and Batchelor, 2001).

1.1.2.4 Boundary Lubrication

Boundary lubrication occurs when a complete fluid film does not develop between potentially rubbing surfaces, the film thickness may be reduced causing temporary dry contact between wear surface high points or asperities. Boundary lubrication takes place in the case of insufficient fluid film.

The increase of the contact pressure beyond elastohydrodynamic lubrication conditions causes a plastic deformation at the contacting asperities and an increase at the number of the contacts as well as a decrease at the fluid film thickness. When the average fluid film thickness falls below the average relative surface roughness, surface contact becomes a major part of the load supporting system and mechanical interactions of these contacts produce wear, deformation, abrasion, adhesion, and fatigue under dry sliding conditions. Furthermore chemical reactions between the lubricant molecules and the asperity surface, due to frictional heating, often produce a boundary chemical film which can be either beneficial or detrimental in terms of wear and the combination of the load sharing by the asperities and the occurrence of chemical reactions constitutes the lubrication regime commonly referred to as the boundary lubrication regime.

Boundary lubrication conditions force the interactions between the two surfaces to take place in the form of asperities colliding with each other and these collisions produce a wide range of consequences at the asperity level, from elastic deformation to plastic deformation to fracture. These collisions produce friction, heat, and sometimes wear. Chemical reactions between lubricant molecules and surfaces usually accompany such collisions producing organic and inorganic surface films and it has long been thought that surface films protect against wear (Bhushan, 2001).

1.1.3 Surface Texture Parameters

Surface geometry has to be measured due to prediction of the component performance and control of the manufacturing process. Every surface has some form of texture which is generated by a combination of the factors such as the micro structure of the material, the action of the cutting tool of the material, the instability in the cutting tool, the errors in machine tool guide ways and the deformations due to stress patterns in the component.

Surface texture parameters can be separated into three basic types:

1. Amplitude parameters
2. Spacing parameters
3. Hybrid parameters

The purpose of a parameter is to apply a number which can characterize a certain aspect of the surface, and hence remove the need for subjective operator assessment. However it is impossible to completely characterize a surface with a single parameter, therefore a combination of the above parameters are normally used. Some of the parameters have more specific uses than others, although they should not be used in isolation to control a specific requirement.

In order to investigate the effects of cylinder bore surface texture on lube oil consumption, it is necessary to comprehend related surface texture parameters. “Arithmetic average” (**Ra**) is the average of the roughness profile from its mean value. “Average Peak-to-valley Profile Roughness” (**Rz**) is measured on an unfiltered profile only and is numerically the average height difference between the five highest peaks and the five lowest valleys within the assessment length where vertical and horizontal thresholds have to be exceeded. Several hybrid surface parameters have also been effective on the analysis. These parameters are combinations of spacing and roughness parameters of the surface profile. “Core Roughness Depth” (**Rk**) is the depth of the roughness core profile. This is the working part of the surface, and after the initial run-in period, carries the load and influence wear and friction performance of the running surfaces. “Reduced Peak Height” (**Rpk**) is the top portion of the surface that will be worn away in the run-in period. “Reduced Valley Depth” (**Rvk**) is the lowest part of the surface that retains lubricant. “Peak Material Component” (**Mr1**) is the material ratio at which Rpk and Rk meet. It represents the upper limit of the core roughness profile. Similarly, “Valley Material Component” (**Mr2**) is the material ratio at which Rvk and Rk meet. It represents the lower limit of the core roughness profile. These parameters are derived from the bearing ratio plot as schematically shown in Figure 1.5. Bearing ratio is the length of material surface (expressed as a percentage of the evaluation length) at a depth below the highest peak. Bearing ratio curve contains all the amplitude information of a profile and its shape can provide detailed information about a surface. A detailed work on the effects of cylinder bore finish on oil consumption was performed by Hill using radioactive tracer and level based measurement systems (Hill, 2001). It was reported in this study that the surface finish parameter with the best correlation to oil consumption was oil retention volume which is the bearing ratio curve area defined

by Rvk and $Mr2$. It is concluded that, oil retention volume is found to be the critical parameter that should be controlled to minimize oil consumption.

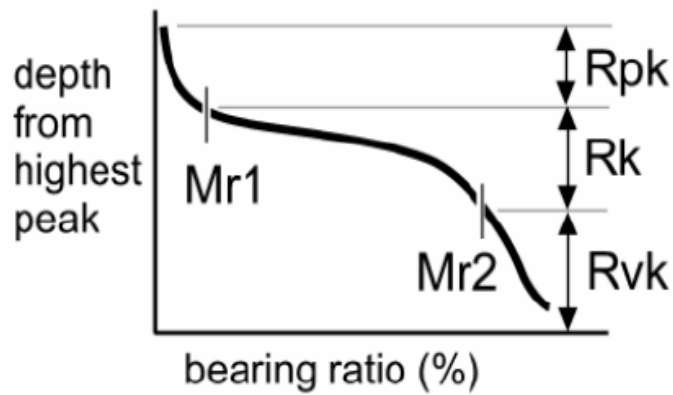


Figure 1.5 Schematic of Bearing Ratio Plot

1.2 Laser Structuring

Tribological functional properties are decisively determined by the surface structure of highly stressed components sliding on each other. The wear behavior of these component surfaces in different fields of application depends on the complex interaction of numerous influence factors, which include the component stress, the kinematic conditions, the combination of materials, the lubricant properties as well as precisely the surface topography of the sliding surfaces. The optimization of such tribological systems can distinctly improve the behavior in application and the service life.

The piston ring/cylinder working surface system constitutes a tribological system in a combustion engine. In order to improve the tribological properties, laser beams are used to produce micro structures in the honed surface of the cylinder working surface, which act as a micro pressure chamber system. Thus the oil consumption and the emission of combustion engines can be reduced. The reduction of the friction loss reduces wear which increases the service life of the engines.

Laser structuring process is also used on tribological function surfaces on bearings of moveable components and forming tools. In these cases the aim is also to minimize the friction and thus the wear, increasing the service life or durability, respectively.

1.2.1 Laser Structuring of Cylinder Working Surfaces

Increasing requirements must be fulfilled by modern highly stressed combustion engines, when issues such as oil consumption and emissions are taken into consideration. Prolongation of the oil change intervals is needed although emission limitations become stringent. Use of modern injection systems enabled lower engine emissions in the past. The high injection pressures and an optimized injection course led to an improvement of the mixture formation and combustion, and thus to a reduction of the fuel consumption and a reduced formation of emission at the same time. However the oil consumption which is responsible for HC and particle emissions could not be reduced to a large extent. Thus, there is an increase of the percentage of emissions resulting from the lubricating oil in the last few years. To achieve further reduction in oil consumption, special attention is directed to the piston group - consisting of the components of piston, piston ring and cylinder working surface - as this is the decisive point of origin for the oil consumption (Gehring GmbH & Co. KG Technical Brochure, 2002). Moreover, the piston group has a share of up to 50 percent in the overall friction in a reciprocating internal combustion engine (Gehring GmbH & Co. KG Technical Brochure, 2002). By focusing on this area, friction loss can be reduced, the efficiency of the engine can be increased and thus the fuel consumption can be reduced. Therefore, the tribological system of the piston group – and here in particular the friction group of piston ring and cylinder working surface – has an extraordinary significance.

In the piston ring/cylinder working surface system, extreme conditions such as temperature and pressure occurs due to continuous change in speeds and loads.

The areas with a high relative speed permit a hydrodynamic pressure build-up in the annular gap provided sufficient oil is present. The areas with lower speed and the extreme case of dead-center position with a standstill of the movement are subjected to especially high loads. Special attention has to be given to the upper dead center in the work cycle as here the highest stress is found due to the ignition (Gehring GmbH & Co. KG Technical Brochure, 2002). Applying laser structures to the surface of the cylinder working surface, lubricating conditions can be optimized in this area.

1.2.2 Machining the Cylinder Working Surfaces

Running properties of an engine are influenced by decisively the material (macro geometry) as well as the surface structure (micro geometry). The adhesion of the oil to the working surface is provided by the surface structure for sufficient lubrication or complete separation of the friction partners involved in order to permit a reliable and low-wear operation for all operating conditions.

The manufacturing method now used all over the world for finish machining cylinder working surfaces, for example for the production of the macro and micro geometries, is honing. After fine boring, pre and finish honing as a two stage process or plateau honing as a three-stage honing process are applied as rule (Gehring GmbH & Co. KG Technical Brochure, 2002). However, often the plateau surface, which is difficult to control from a production-orientated point, is preferred.

The honed surface has two functions basically which are providing a high carrying capacity thus ensuring good sliding properties of the component through a high material carrying capacity with a low cutting depth (low roughness) and developing an open structure to ensure the adhesion of the lubricant, which would necessitate a rough surface. These two functions can be combined by providing a rough base profile with a fine surface relief which is called plateau. The ideal structuring of the surface is generated by means of laser beams. Thus, the target of the laser structuring process is to create surface topographies with adequate lubricant retention volumes, a high lubricant dwell time as well as the encouragement of a hydrodynamic pressure buildup.

Since the distribution of the grain size and the grain distribution in the honing stone structure are unavoidable, irregularities occur in the surface topography in conventional plateau honing. In order to produce engine-specific surfaces with designable relief the width, depth, length and space between the rough surface relief and the superimposed fine relief must be manufactured. This should be possible with different designs and shapes along the working surface as well (Gehring GmbH & Co. KG Technical Brochure, 2002).

The demands for a functional surface relief can be met with a high flexibility by means of laser structuring processes. “Laser honing” process is characterized by a combination

of the honing and laser techniques, and fulfills the target ideas the engine developers have had for a long time already. A new surface texturing technique forming micro structure in the cylinder working surface is introduced in order to optimize the tribological system of piston and cylinder working area. Different dimple shapes are shown in Figure 1.6.

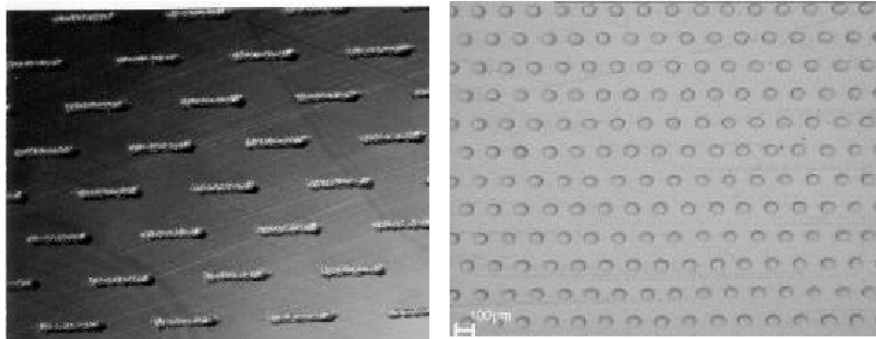


Figure 1.6 Different Dimple Shapes

In this technique, the arrangement of lubricant pockets has great importance due to task of avoiding the possibility of lubricant getting into combustion chamber. Since the structure enables the lubricant to remain in the effective position for a longer period of time, a hydrodynamic pressure is built up. In an ideal case, there is no relative movement between the lubricant and the basic solid and the counter body caused by adhesion forces. The move of liquid parts counteracts wear. In application the structure has to be independent of the direction owing to the movement of sliding surfaces in alternating directions. As a rule cup or pocket structure is applied. The dimensions of the recesses are defined as 40 to 80 μm for width and diameter respectively and the depth of the recesses must be between 5 and 25 μm . This structuring process in cylinder working surfaces in combustion engines is conducted by the basic set-up of the machining plant corresponds to a honing machine. The rotating and lifting movement of the laser head is carried out by the spindle. Beam guiding in a laser machining plant and in a laser head system is presented in Figure 1.7.

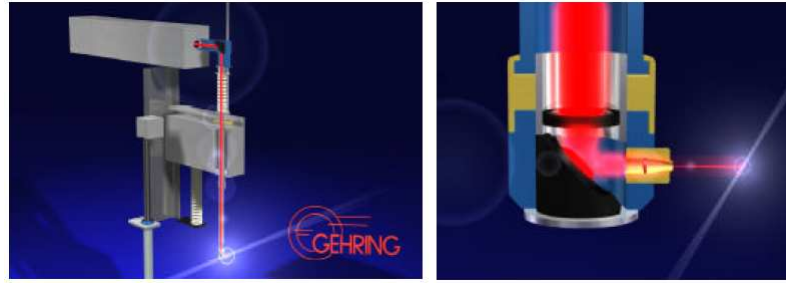


Figure 1.7 Beam Guiding in a Laser Machining Plant and in a Laser Head System

In this system, laser beam source is a Q-switch Nd:YAG laser and the irradiation pass the beam guiding system to the laser head. The head focuses the laser irradiation and there occurs 90° deflection onto the cylinder working surface. Very high intensities in the focusing plane cause the ablation of material. The finishing process consists of four work stages – the conventional pre and intermediate honing, the laser structuring and the finish honing. The process sequence of laser structuring is given in Figure 1.8.

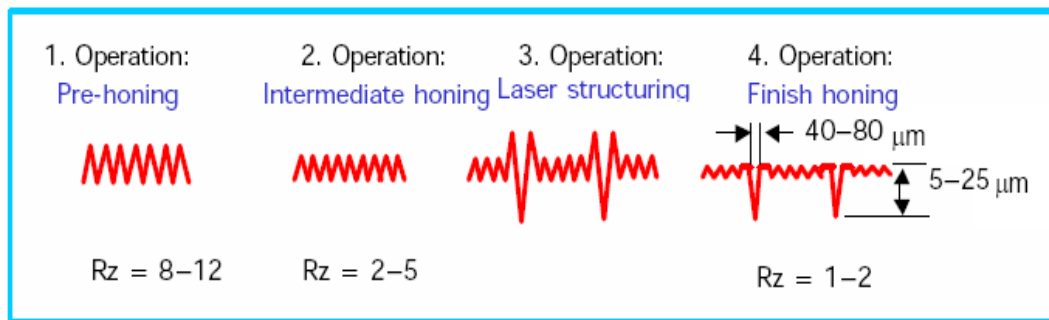


Figure 1.8 Process Sequence of Laser Structuring of Cylinder Working Surfaces

Pre and intermediate honing provides improvement of macro structure almost to the final accuracy. Hence the initial surface for laser structuring of the borehole is completed and subsequently the application of the defined laser structure takes place. Since laser machining process leaves over burr deposits finish honing process is required thus an extremely fine sliding surface of 1 to 2 μm Rz is obtained.

Fundamental investigations have been carried out fundamental investigations in order to improve the understanding of the relationships in the area of the piston ring/cylinder working surface both on standard honed and laser structured engine blocks.

According to the investigations, it is shown that high cylinder pressure in the upper dead center causes the height of the oil film to decrease considerably, subsequently to increase again at the beginning of the downward movement. Since the lubricating film is interrupted in the dead center due to high cylinder pressures causing mixed friction, wear is observed. The gap width decreases back to the previous level, outside of the laser pocket field which can not be found in unstructured working surfaces.

It is very distinct that the increase of the oil film thickness provides the piston ring to float in the area of the laser structure due to forming hydrodynamic pressure. A considerable improvement of the lubricating conditions due to reduction of knuckle wear enables longer service life of the engines.

Since roughness causes distinct reduction of the oil consumption, the oil retention volume of the honed cylinder working surface is considerably lower, whereby the laser structure protects the highly stressed areas of the engine against failure due to lack of lubrication.

1.2.3 Laser Structuring of Other Functional Surfaces

Apart from the application of laser structuring processes on piston working surfaces of combustion engines, laser structuring is used in other working surfaces which are listed below in order to improve their tribological behaviour.

- Face of the large connecting rod top
- Small connecting rod top
- Piston bolt
- Crank shaft
- Sliding bearing
- Forming and punching tools
- Drawing tools

In the connecting rod case, application of different wear layers could not solve severe wearing problems occurred on the face of the large connecting rod top of a highly

stressed engine. Subsequently, the defined pocket structure for the surface provided a considerable reduction of wear.

Forming tools are also subjected to considerable stress. By means of a structured surface, the service life of these tools could be increased.

Application of laser structuring may be considered safe in moving components, particularly in the area of bearings, in order to minimize friction and wear.

1.3 Oil Transport Mechanisms of IC Engines

1.3.1 Piston-Ring Pack

The ring and groove geometry with temperature and pressure conditions at the interface between piston and liner constitute leading factors for oil flow. The effects of these parameters on oil transport in the piston ring pack were not clear due to lack of data on this subject. Therefore a new technique is needed to have accurate prediction of oil consumption.

For the oil transport of crown land, two mechanisms were determined. First mechanism showed that, oil flows through the top ring groove in all engine conditions at each time that oil accumulates on the second land. This type of oil transport refers to top ring axial motion. Top ring up scraping is the main oil supply mechanism to the crown land at high engine speed and low load which is known as second mechanism.

The main path of oil flow at the piston liner interface for a test engine is identified by Thiourad, Tian and Hart (1998). Top ring scrapes down the part of oil, which is left on the liner by oil control ring, permitting it to flow to the second land. Subsequently, part of the oil is transported as liquid oil through the ring groove or as mist through the top ring gap to the crown land from the second land where it accumulates. On the other hand oil flow by gas dragging toward the scraper ring gap and then is broken into mist as flowing through the gap. Part of oil is scraped up by the top ring and transported to the combustion chamber due to increasing engine speed.

1.3.1.1 Oil Transport through the Ring Grooves

There are three steps of oil flow through the ring grooves which are caused by various driving forces. Firstly, the oil must be driven from one land into a ring/groove side clearance. Subsequently the oil is transported from the clearance on one side of the ring to the clearance on the other side through the back of the ring. Finally, oil must be driven from ring/groove clearance of the other side of the ring to the adjacent piston land.

Since the oil flows into and out of the ring grooves reach equilibrium, the amount of the oil that accumulated in the back of the ring stays the same. Hence, the rate of oil transport through the ring grooves may be fully characterized by determining the oil flow mechanism between the lands and grooves. The large volume located at the back of the ring may be introduced as a buffer region which can affect the net oil flow through the ring groove (Thirouard and Tian, 2003).

1.3.1.2 Oil Transport from the Piston Land into the Grooves

There exist three potential oil transport mechanisms from the piston lands to the ring/groove side clearances (Thirouard, 2001).

1. Ring mechanical pumping
2. Dragging action of the gas flow from the piston land to the groove.
3. Shear driven oil flow due to lateral motion of the piston relative to the rings.

Ring mechanical pumping: Ring position which is relative to the entrance of the ring groove clearances changes according to rings twist and move up and down in the grooves. As the ring moves away from the groove, oil may accumulate in the area of the ring groove clearance depending on the timing of the ring motion and inertia-driven oil flow. Subsequently, part of the oil accumulated on the side of the ring will be driven into the gap opening between the ring and groove (Thirouard and Tian, 2003).

Gas dragging from the lands to the grooves in the axial direction: The instantaneous oil flow rate which is generated by the gas flow in the axial direction is not as high as the rate which is generated by the inertia force when ring flutter takes place. Thus the axial oil distribution of lands is not significantly affected by the dragging

action of gases between the lands and the grooves. On the other hand, the oil flow, which is generated by the gas flow when ring flutters, is unidirectional. Furthermore, considerable rate of oil is remained on the piston land (Thirouard and Tian, 2003).

Lateral motion of the piston relative to the rings: Lateral motion of piston relative to the rings causes shear action which initiates the oil transportation inside the ring/groove clearances, as it can be seen in Figure 1.9. Oil is expected to exist adjacent to the ring/groove clearance for this sort of transportation. The timing of the piston secondary motion and the inertia force is used for determining the amount of oil available in front of the ring/groove clearance at the time piston moves from side to side. The volume of oil transported inside will be controlled by the amount of oil accumulated in front of the ring/groove clearance when the thickness is less than the amplitude. Moreover, the amount of oil transported into the ring groove is affected by the clearance between ring and groove and consequently by the ring position (Thirouard and Tian, 2003).

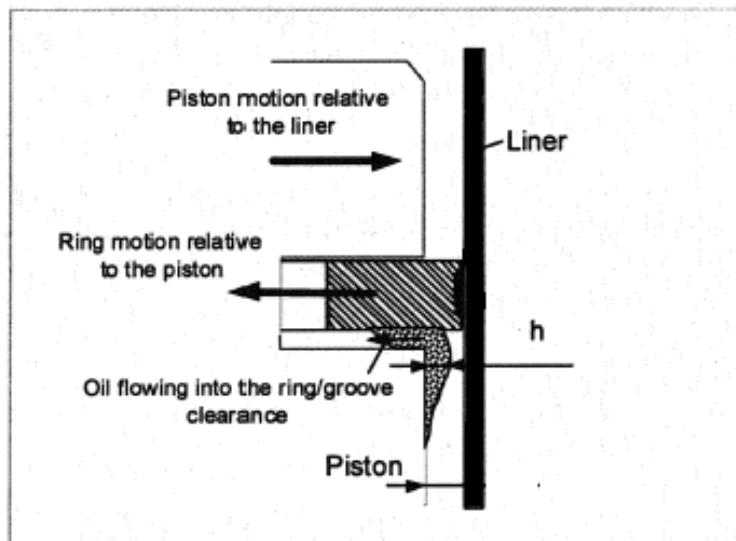


Figure 1.9 Description of the Oil Transport into the Ring Groove (Thirouard and Tian, 2003)

To sum up, experiment and observations which are conducted by Thirouard and Tian (2003), it can be asserted that two mechanisms were determined as the potential modes of the oil transport from the piston land to the ring/groove clearances (Thirouard and Tian, 2003) :

1. Ring pumping mechanism which is available for all of three rings.
2. Flow caused by the lateral motion of the piston relative to the rings.

Oil adjacent to the ring groove clearance during a specific period of engine cycle affects these two mechanisms significantly. Since the repartition of the oil along the axial direction of the piston lands is governed by the inertia force, the rate at which the oil is transported into the ring groove is strongly dependent on the timing of the inertia force in regards to ring twist, ring lift and piston secondary motion. (Thirouard and Tian, 2003)

1.3.1.3 Oil Transport from the Grooves to the Lands

Two potential mechanisms of oil transport from the ring/groove clearances to the lands were identified and investigated by Thirouard and Tian (2003).

1. Ring squeezing
2. Gas flow dragging in the ring/groove clearances.

Ring squeezing: When one ring is moving toward one side of its groove, part of the oil layer covering the side of the groove and the ring is being squeezed out of the ring/groove clearance and the oil is squeezed toward both the inside and the outside of the groove (Thirouard and Tian, 2003). This sort of flow maintains a net transport of oil from the ring groove to the piston lands. This mechanism indicates main mode of oil transportation from the ring grooves to the piston lands in most engine operating conditions.

Gas flow dragging in the ring/groove clearances: The gas flow between the grooves and the piston lands has the potential to drag oil covering the sides of the ring/groove clearances and the lands (Thirouard and Tian, 2003).

In conclusion, the oil transportation rate from the ring grooves to the piston lands by means of gas flow dragging action through the ring groove clearances is small for the top ring but it should not be neglected. This mechanism is substantially related with ring flutter and significant for any groove where the ring flutters. Moreover it is generally smaller than the rate of oil squeeze (Thirouard and Tian, 2003).

1.3.1.4 Oil Flow through the Ring Gaps

For most engine operating conditions, ring gaps are found to be the major paths of gas flow from the combustion chamber to the crankcase. Yilmaz et al. (2004), underlined that during several periods of the engine cycle, when the second land pressure becomes greater than the combustion chamber pressure, reverse gas flows into the combustion chamber through the top ring gap and around the top ring groove if the top ring loses its stability in the groove. The mechanism is governed especially by the top two rings. Thirouard and Tian (2003), also investigated and characterized oil flows through the piston ring gap for various engine running conditions. The mechanism is shown in figure 1.10.

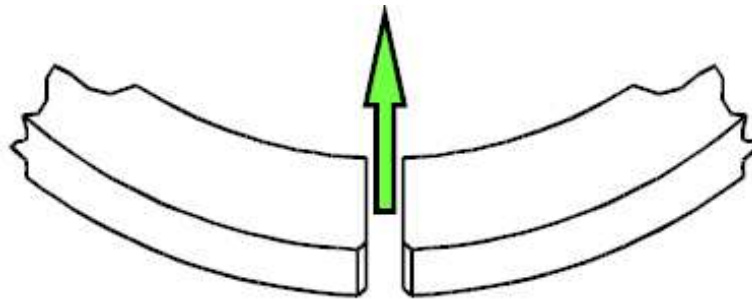


Figure 1.10 Oil Blow through End Gap into the Combustion Chamber (Yilmaz et al., 2004)

1.3.2 Turbocharger

Turbocharger is also a significant contributor to total oil consumption which is lubricated by the same lubricant of the engine circuit in order to provide a relatively simple system, easier maintenance and lower cost. Excessive bearing clearance is one of the oil consumption mechanisms of turbocharger. Lubrication is required by the journal bearings which are also subjected to high loads during driving operation. If the bearings in the turbocharger, illustrated in Figure 1.11, are worn then the impeller seals will no longer be able to provide a perfect seal because of the increased bearing clearance (0.02-0.05 mm) (Manni et al., 2002). Engine lubricating oil is then sucked in and burned in the combustion chamber together with the air/fuel mixture.

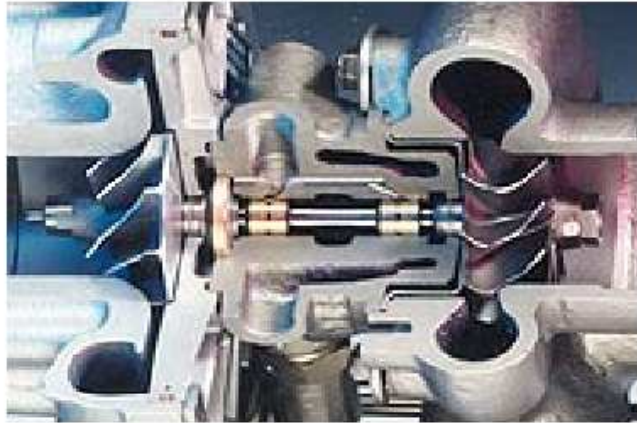


Figure 1.11 Turbocharger Bearing System (Cutaway Model)

1.3.3 Valve Guide Leakage

The lubricating oil is carried from the cylinder head through the valve guide into the intake port when intake manifold pressure is adequately below the atmospheric pressure. The schematic of valve guide leakage is shown in Figure 1.12. For the earlier spark ignition engines, this mechanism was a major contributor to oil consumption especially during partial loads.

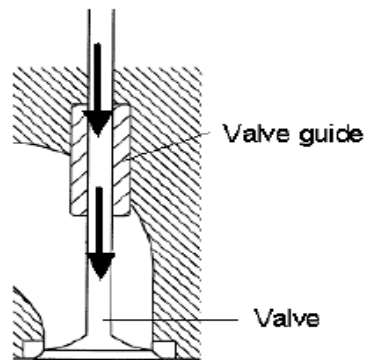


Figure 1.12 Schematic of Valve Guide Leakage

To sum up, the contribution of each oil consumption mechanism which is described above varies with engine operating conditions. The relative importance of each source and mechanism depend on different driving forces for oil transport which change with different design and engine operating parameters. Thus advancement of the

understanding of the characteristics, sources and driving mechanism of oil consumption are required in order to eliminate oil consumption problems.

1.4 Oil Consumption Measurement Methods for Internal Combustion Engines

Various oil consumption measurement methods have been applied over the years. Since determining the oil consumption of an internal combustion engine implies a great challenge, the methods needed to be developed. The classification of oil consumption measurement methods is shown in Figure 1.13.

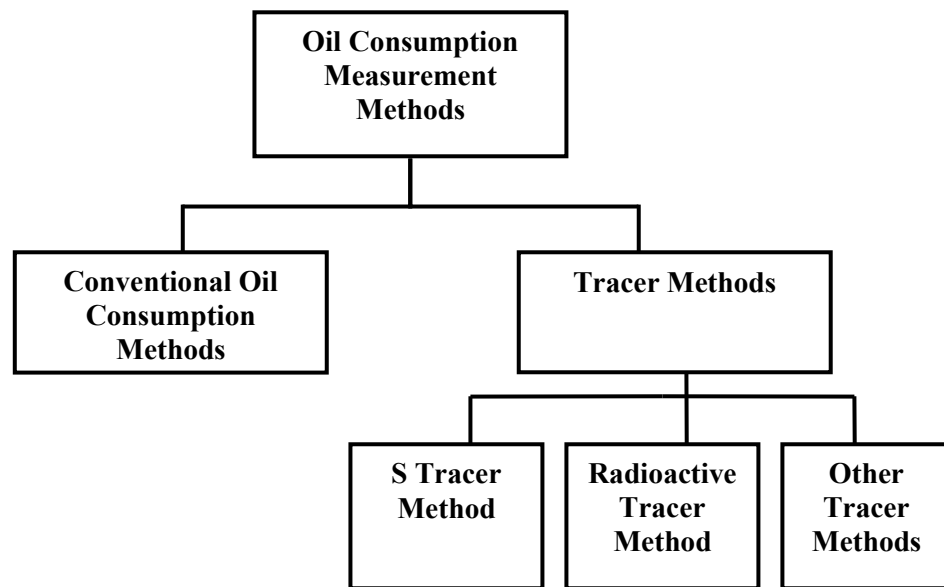


Figure 1.13 The Classification of Oil Consumption Measurement Methods

Conventional methods which are based on gravimetric and volumetric studies constitute the initial efforts in order to measure oil consumption. Subsequently, more advanced methods such as tracer methods have been developed. Tracer method is based on the idea of observing a tracer in the exhaust gas stream during the engine operation. Tracer methods are beneficial due to the possibility of real time oil consumption measurement. There also exist analytical prediction methods which are basically computer simulations providing the prediction of the oil consumption with theoretical calculations. Although there are also some limitations and disadvantages for the lube oil consumption measurement methods depending on the purpose.

1.4.1 Conventional Oil Consumption Measurement Methods

Since there are various techniques of oil consumption measurement, conventional methods, which are still widely used, constitutes fundamental of these methods. Conventional methods are based on gravimetric and volumetric measurements. Simplicity and lower cost are the advantages of the conventional methods however they are more inaccurate and more operator dependent systems. Moreover, it takes a long period of time to obtain meaningful data with conventional methods.

Dip Stick Method or Level Top up method: This method is the simplest method however it is the least accurate one for measurement of the oil consumption. In this method, the system is filled with oil to a specific level on the dipstick. After engine is run and oil is consumed, the engine is shutdown and allowed to cool. Subsequently, the oil level is measured and a determined quantity of oil is added in order to bring the oil level back up to the initial level. Finally, the oil added is considered the amount of oil consumed (Weng and Richardson, 2000)

Since the system is very simple and does not need any extra equipment, it becomes practical. However getting accurate results takes too long time engine operation. Oil leaks which are also measured as oil consumption and operator dependent operation necessity are the major drawbacks of the system (Weng and Richardson, 2000).

Drain and Weigh System: The drain and weigh system is found to be a reasonably simple system for the determination of lube oil consumption due to its principle of operation. In this technique, a measured amount of oil is put in the engine and then the engine is operated for a determined period of time. Sequentially, the oil is completely drained from the engine in order to be weighed. The difference in oil weight gives the oil consumption (Weng and Richardson, 2000).

The main advantages of the system is simplicity and low cost. On the other hand tests take long time to obtain accurate results. Furthermore, the results are affected by the consistency of oil draining process from the engine. Oil leaks may also be measured as oil consumption. Besides, the system is operator dependent (Weng and Richardson, 2000).

Oil Pump System: In this technique, an oil drain tube is connected to the engine at a determined position on the oil pan. Used oil is drained into a vessel by means of this tube. Subsequently, oil is pumped from the vessel back into the engine. Since oil is being continuously circulated between the oil cart and the engine, the system design enables the oil to be at the oil drain tube location. Fresh oil added into the vessel for used oil from the tank above it, when the oil level starts to decrease below a specific amount. The weight of the two tanks is measured continuously in order to determine total decrease in the weight of the two tanks which gives the amount of oil consumption (Weng and Richardson, 2000).

Since easy setup is available due to the possibility of fixing the oil level by means of oil drain tube, the technique becomes advantageous. On the other hand, system is complex, large in size, does not permit oil consumption measurement during cyclic engine operation and measures oil leaks in the engine as oil consumption. The system which is also used by Federal-Mogul as drain and weight system is shown in the Figure 1.14.

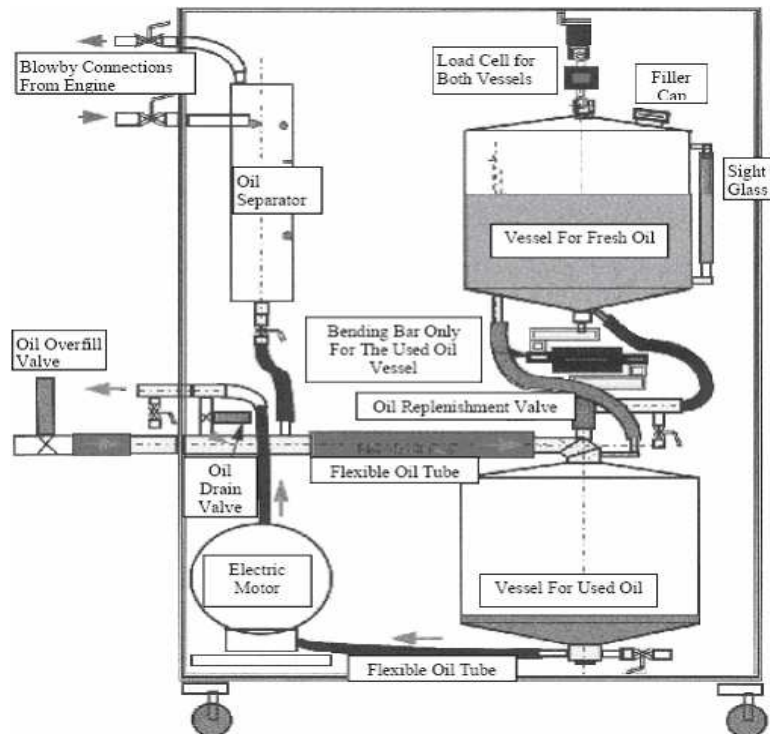


Figure 1.14 Schematic of Oil and Pump System (Weng and Richardson, 2000)

Oil Level Change Rate System: The system is also commercially available as AVL 403 and AVL 403S. The system is shown schematically in the Figure 1.15. Since a tube which connects the engine and the float tank is maintained, the oil level is the same in both of them. There occurs same pressure above the oil in both the engine and oil cart by means of an equalization or vent tube. The system must be calibrated before the engine operation. As determined amounts of oil are put in the sump, the corresponding level measurement from the capacitance sensor is recorded in order to have calibration. Calibration can be made either manually or automatically due to selection opportunity created by AVL. As the engine consumes oil during the operation, the oil level decreases in both the engine and the oil cart float tank. In that case, calibration is used for determination the of oil amount that is present in the system. Finally, oil consumption is calculated by the change in measured oil from the sump (Weng and Richardson, 2000).

The system is not a complex one and calibration of the system is also simple. Another advantage of the system is possibility of short time period for stabilization. On the other hand, the system also has drawbacks. Oil conditions such as temperature, aeration or soot may affect the results when the calibration oil level sump volume is used. Moreover changes in the shape of the oil pan may affect the accuracy of the system since the calibration depends on the shape of the oil pan. Also in this system, oil leaks in the engine are measured as oil consumption. High cost is another disadvantage of the system and since usage of constant level principle needs appropriate oil level, there may be caused problems in setting the appropriate level (Weng and Richardson, 2000).

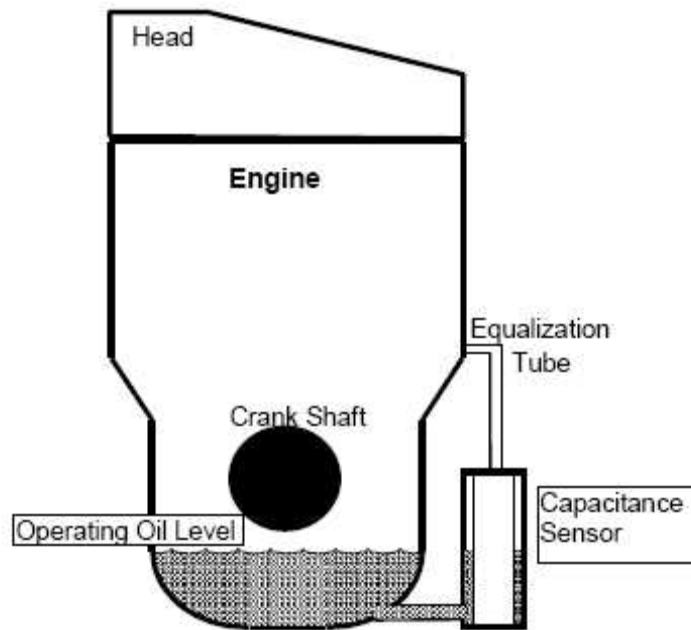


Figure 1.15 Oil Level Change Rate Oil Consumption Measurement Device

Gravity Fed System: This system is used constantly in the development of diesel engines and it was used around 1984 for the first time. In this system, the oil level in the engine and the car are the same by means of a tube that connects the oil cart float tank to the oil pan of the engine which is showed in Figure 1.16. Therefore, oil moves constantly back and forth between the engine and the cart. Same pressure value above the oil in both the engine and oil cart is obtained since the equalization or vent tube exist in the system. Since the oil level decreases in both the engine and the oil cart float tank when the engine consumes oil, the float falls opening a needle valve that permits oil to drain from the weigh tank. Then, the weight of weigh tank decreases. In order to have the oil drained properly from the weigh tank to the float tank, there should be a pressure balance by means of an equalization tube or vent tube in the system. The oil coming from the weigh tank causes the oil level to increase again raising the float, closing the needle and stopping the oil flow from the weigh tank subsequently. Finally, the amount of the oil consumption is measured by the change in the weight of the weigh tanks (Weng and Richardson, 2000).

Both of the system setup and calibration of the system are reasonably simple. Furthermore the method is relatively cheap. On the other hand, the set up of the system

is considerably significant due to incorrect results measured in the case of improper set up. Operator dependence is another disadvantage of the system. Moreover, oil leaks in the engine are measured as oil consumption. The system needs long time for stabilization (Weng and Richardson, 2000).

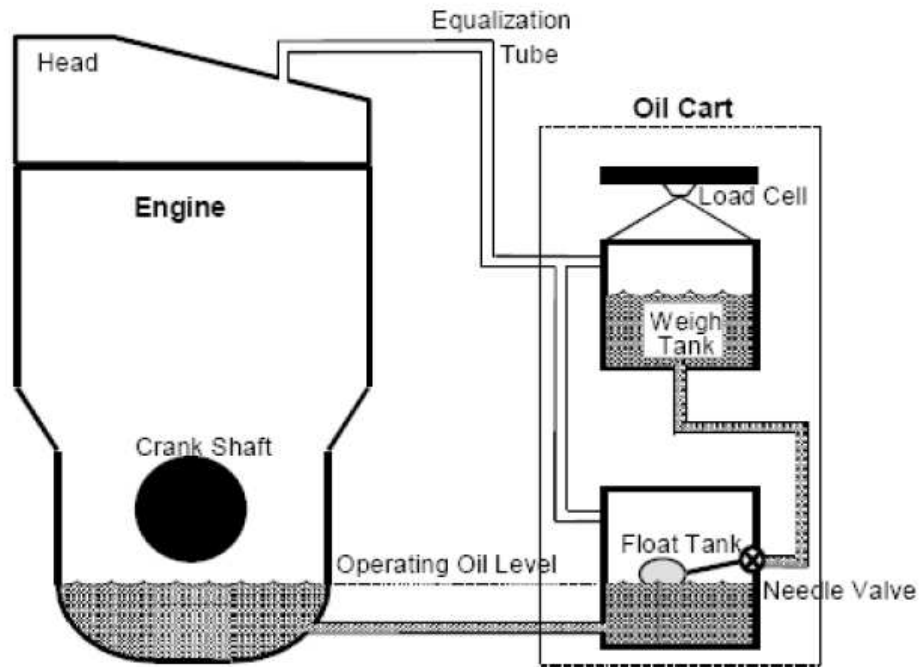


Figure 1.16 Gravity Fed Measurement System (Weng and Richardson, 2000)

Smart Oil Consumption Measurement System: This system has been developed in order to resolve the disadvantages of conventional oil consumption measurement methods by Weng and Richardson (2000). This system includes the conventional techniques used in the “Gravity Fed Oil Consumption Measurement System” and in the “Oil Level Change Rate System”. On the other hand, the system has been improved in order to obtain easier system maintenance and setup. The principle of the measurement method is established by operating the engine at stabilized conditions and stabilized oil level in the oil pan. In other words, engine is run at constant speed with constant load in order to include a cycle test which causes the major difference between the Smart Oil Consumption Measuring System and conventional oil consumption measurement methods. Since oil is consumed in the engine, to obtain a constant level, fresh oil is constantly added by the system to the oil pan. Fresh oil flow rate gives the oil

consumption rate of the engine. The diagram of the system is illustrated in the Figure 1.17. A level sensor is used for the measurement of the level in the oil pan or in the oil fill cylinder. The oil level is controlled by PID algorithm.

There are several advantages of the system. First of all, the system is reasonably simple in concept and calibration. Controlling of oil level setup is maintained automatically. Moreover system is available for measurement of oil consumption at cyclic operations and the measurement takes relatively less time when compared with conventional measurement methods. It is also less operator-dependent. However, the measurement time of this method is greater than measurement time of real time oil consumption methods and oil leaks in the engine are again measured as oil consumption.

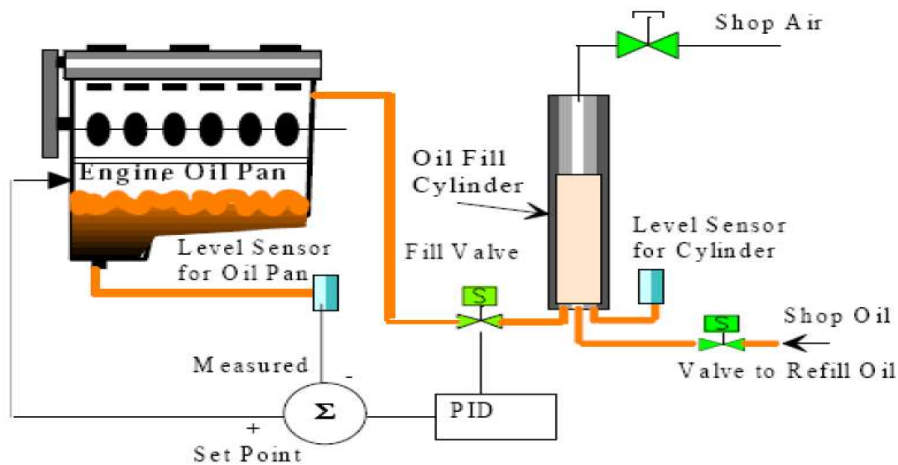


Figure 1.17 Smart Oil Consumption Measurement (Weng and Richardson, 2000)

AVL Oil Consumption Meter 406: The AVL Oil Consumption Meter 406 which provides quick automatic measurement of IC engine oil consumption is a compact, mobile measurement system. The device consists of a measuring vessel, a refilling tank, a gear pump and control electronics. In the system, the oil is pumped off either constantly or to a determined level through a modified oil dipstick or the oil drain plug. Subsequently, the oil is stored in a special tank in the AVL measurement system and a high precision pressure sensor is used for weighing. The measurements can also be obtained while the engine is running. Hence a substantial reduction in measurement time is provided. The oil is pumped back into the engine after measurement takes place. This

technique is used in the areas such as engine test beds oil testing, endurance testing and quality testing (AVL Internet, 2006). The system is illustrated in Figure 1.18.

In this system, the lubricating oil is pumped with a gear pump out of the sump into the measuring vessel where it is weighed and then pumped back again. Oil consumption results from the difference of successive measurement cycles. When it is needed, clean oil can be refilled from the refilling tank. The process control and the communication with the test bed automatic system are achieved by means of control electronics. The engine oil is drained over a dirt trap in order to avoid soiling. The pressure sensor which is present in the measuring vessel needs a small amount of remaining oil for protection against extremely higher temperatures.

The system enables time saving compared to conventional drain and weigh method. It also provides simple hybrid integration in an automation system. Simple parameterisation is also achieved. Moreover, measurement of oil consumption during engine operation is another advantage of the system. Risk of soiling does not exist with drained oil compared to the drain and weigh method

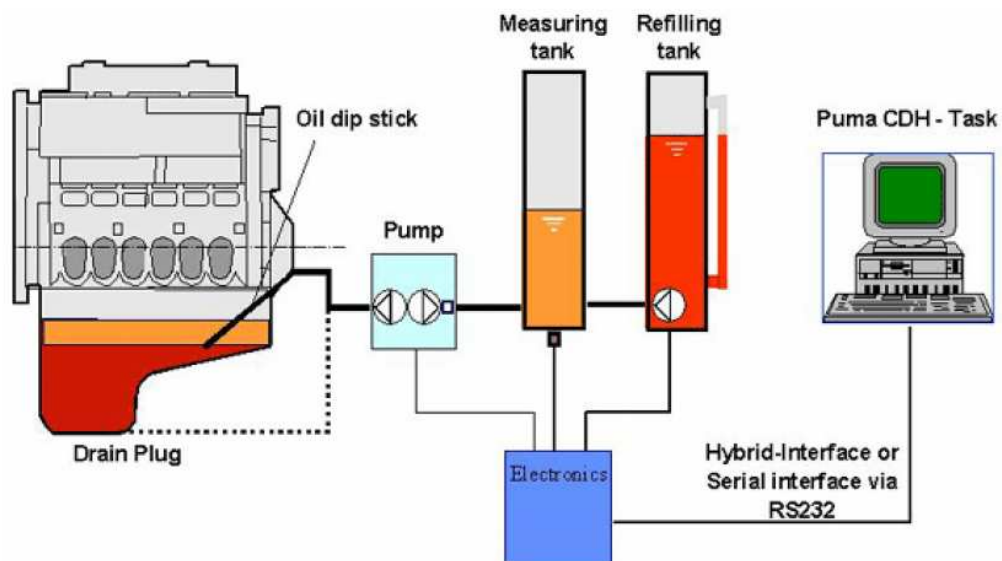


Figure 1.18 AVL 406 Oil Consumption Meter (AVL Internet, 2006)

1.4.2 Tracer Methods

Engine oil consumption becomes more important today due to the constraints such as customer satisfaction through oil change and oil refill intervals, engine out emissions through particulate and hydrocarbon emissions and also tailpipe emissions through chemical poisoning of the exhaust gas after treatment systems by oil additives. Therefore oil consumption control has priority considering the expected increase of pressure from these constraints in the near future.

Although easier techniques listed above can be appropriate development tools, they suffer from low resolution in time and low accuracy due to the uncertainties in the lubricant entrained air and uncertainties in the lubricant composition caused by dissolved particulate matter or fuel components (Haas and Geiger, 1994).

Tracer techniques such as radioactive tracer, SO₂ tracer and other tracer are the most advanced techniques for oil consumption measurement. A characteristic of this technique is the possibility for obtaining high resolution in time. The SO₂ tracer technique is found to be the fastest technique available for obtaining data. Moreover, there also exist local techniques such as 2D Laser Induced Fluorescence technique (LIF), assisted by advanced computer models, is providing valuable insight into detailed mechanisms of oil consumption (Froelund et al., 1999).

Tracer methods are based on the principle of sensitive measurement of tracer material in the exhaust gas. In this method, lubricating oil is labeled with a known amount of tracer. An analyzer detects the tracer in the exhaust gas stream as consumed oil leaves the engine. Finally, oil consumption is calculated by means of the tracer concentration in the exhaust gas, in test oil and in test fuel using chemical mass balance. In addition to this, fuels with low radioactive elements are used in the technique and known content of tracer material is employed. Several tracer materials such as sulfur, tritium, bromine, germanium, magnesium, pyrene, calcium and radioactive elements are used as declared in the literature.

Fast measurement and possibility of transient oil consumption measurement are the advantages of the system. Moreover oil leaks in the engine are not measured as oil

consumption. Therefore the method enables relatively sensitive and accurate results. Oil consumption can be measured from each cylinder individually by this method.

However, there are also obstacles of the method such as complexity of oil consumption calculations after measurement. Furthermore, special fuel and lubricating oil must be required for the system. Some uncertainties may be caused due to specially treated oil performance. The system also makes the measurement of intake airflow and fuel consumptions necessary in order to determine the oil consumption rate. The result may change with the ambient conditions thus they must be taken into account seriously. In addition to this, special safety considerations are required for radioactive tracer elements.

Sulfur (S) Tracer Method: Sulfur (S) or sulfur dioxide (SO_2) tracer method is the most common and advanced technique in oil consumption measurement. This technique is originally introduced since it could provide a superior accuracy and resolution on time. Working principle of the SO_2 -technique is to operate the engine on a sulfur-containing lubricant and a low sulfur content fuel. The part of sulfur which enters the engine combustion chamber is oxidized to form SO_x (mostly SO_2). Subsequently it is emitted into the atmosphere with exhaust gases. Hence, SO_x emissions from the engine are directly proportional to both fuel and lube oil S content and their consumption. Lube oil is labeled with S element which is already present in itself. As S burns with lubricant in the combustion chamber, SO_2 is formed. Since SO_2 leaves the engine in the exhaust stream, engine oil consumption can be calculated on the basis of SO_2 concentration measured in the exhaust gas and S concentration of fuel and lube oil. Engine air flow and fuel consumption are also required to be measured instantaneously during the tests.

The most important advantages of the S tracer method are capability of real time oil consumption measurement. Additionally, the method enables the possibility of each individual cylinder oil consumption measurement. Fast and accurate results are obtained when compared with conventional methods. Moreover modification on the test engine is unnecessary.

In order to have oil consumption measurement with this method, a reliable and fast response sampling train system and sensitive SO_2 detection analyzer are required.

Besides, high S content lube oil and low (or zero) S content fuel are other major demands of the system. In addition to this, very high S concentration in the lubricant may cause thermal instabilities.

Radioactive Tracer Method: In order to meet the need in online and sensitive tool, an alternative methodology was developed for monitoring the oil consumption on internal engines. This method is based on lubricant labeling using innovative radiotracer compounds that are representative of the distillation interval of the base oil. During engine operation, the tracer is burned proportionally to the lubricant and a monitoring system is installed in the exhaust line where the marker is trapped. The measurement enables detection of the signal (gamma rays) which is emitted by the radioactive tracer. This signal is automatically converted into terms of oil consumption. The amount of oil consumption can be determined by means of mass balance calculation.

Radioactive tracer method is capable for real time oil consumption measurement and cylinder by cylinder oil consumption measurement just like in S tracer method. Moreover, special fuel is unnecessary since the radioactive tracer material is unique in the oil. More sensitive and accurate results can be obtained due to the advantages mentioned above. However the method also has some drawbacks based on its configuration. For instance, special safety considerations are needed due to radioactivity. Moreover the system is relatively expensive and used test oil constitutes a major problem since it forms a radioactive waste for the environment.

Tritium (T) and Bromine (Br) are used as radioactive tracer material in general. However according to Delvigne (2005) advanced equipment including a heavy water condenser system at the engine exhaust is required for usage of Tritium as radioactive tracer material. Furthermore, it is not easy to measure oil consumption instantaneously, because it is complicated to detect the tritium. Therefore, this makes detecting variations in the oil consumption difficult (Schofield, 1995).

1.4.3 Analytical Prediction Studies

During engine development, oil consumption is generally improved upon by repeating engine tests that run for extended period of time. However, due to shortening of development time and reducing development budget, there is strong demand for

establishing a technique for determining the oil consumption without performing engine tests. However, analytical predicting the oil consumption is extremely difficult because oil consumption is currently calculated by using various assumptions and estimations. This is because oil consumption is a complex phenomenon of various factors that are closely connected each other. Especially, the mechanism with which the oil passes by the piston rings and into the combustion chamber is not sufficiently clear (Yamada et al., 2003).

1.5 Literature Survey

Various techniques can be employed for surface texturing however laser surface texturing is the most advanced so far. Laser surface texturing produces a very large number of micro dimples on the surface and each of these micro dimples can serve either as a micro hydrodynamic bearing in cases of starved lubrication conditions or a micro trap for wear debris in either lubricated or dry sliding. In this part, theoretical and experimental studies being made world wide on laser surface texturing is told with their results.

1.5.1 Experimental Studies on Laser Surface Texturing

Etsion and Kligerman (1999) found that the actual shape of the micro-dimple does not play a significant role and that the most significant parameter for optimum load capacity is the ratio of the dimple depth over diameter. The modeling is based on solving the Reynolds equation for the hydrodynamic pressure distribution and finding the average pressure in the sealing dam for various operating conditions. In this study, a high stiffness of the fluid film below a clearance of 1 μm and a very good agreement between theory and experiment was shown.

Etsion (2000) made further testing of actual seals in water showed dramatic reduction of up to 65% in friction torque and face temperature. Similar results of lower friction and face temperature with laser textured seal face were found by Yu et al. (2002) in East China University of Science and Technology and are reported in where textured SiC rings were tested against carbon rings in oil.

Kononenko and Garnov (2000) worked on an extensive research on laser surface texturing at the Institute of Applied Physics of the University of Bern in Switzerland utilizing Q-switched Nd:YAG but mostly femtosecond lasers. This work is mainly aimed at studying the texturing process itself however limited basic tribological tests are also performed in collaboration with researchers at other institutions like CSEM in Neuchatel, Switzerland and elsewhere.

Dumitru and Romano (2000), for example arranged a ball-on-disk test where a small fixed amount of lubricant is provided and the evolution of friction coefficient with sliding distance is monitored. The lifetime of a sample was defined as the distance at which friction starts to increase rapidly. It was found that the lifetime of LST sample disks could be eight times longer than that of untextured samples.

Wang et al. (2001) at Tohoku University used a CO₂ laser to texture SiC surfaces for studying the effect of LST on the transition from hydrodynamic to mixed lubrication regime. Experiments were carried out with a disk and a cylinder configuration loaded axially under water lubrication. Surface texture in the form of micro-pores with a diameter of 150 μm and a depth of about 8–10 μm was tested and compared with untextured specimens. It was found that the critical load for the transition from hydrodynamic to mixed lubrication in the case of the textured specimens was 20% larger than that for the untextured faces.

In a subsequent experimental work, which is performed by Ryk et al. (2002) an experimental study was conducted to evaluate the effect of laser surface texturing in the form of micro dimples in reciprocating automotive components. A plane surface and a real ring/liner were the configurations of the specimens for test rig. Up to 40 and 30 percent of friction reduction was observed in the first and second configurations, respectively. Good correlation was found with the theoretical results of Ronen. Optimum parameters of the laser surface texturing were in good agreement with theoretical predictions. Laser texturing is found to be beneficial over the entire range of the tested flow rates of the lubricant, with optimum dimple depth and low lubricant viscosity. Laser texturing became detrimental with the deepest dimples and low viscosity.

Etsion and Halperin (2002) developed special treatment that enhances hydrostatic effects in high-pressure seals. This treatment consists of applying higher density LST over a portion of the sealing dam adjacent to the high-pressure side and leaving the remaining portion nontextured. The textured portion provides an equivalent larger gap so that the end result is a converging seal gap in the direction of pressure drop, which produces hydrostatic effect. Hence, they proved that the high pressure sealing capability of the textured seals is substantially greater than that of the standard nontextured ones.

Varenberg and Halperin (2002) showed that, LST can reduce friction also in dry contact applications. In this study, 84% reduction in the electrical contact resistance of the textured fretting surfaces compared to the case with nontextured surfaces is provided due to escape of oxide wear debris into the LST micro-dimples.

Volchok and Halperin (2002) conducted a limited number of fretting fatigue tests in order to demonstrate the potential effect of LST on fretting fatigue life. The LST allowed an easier wear debris escape from the fretted zone into the micro-dimples thus, improved the fretting fatigue resistance and almost doubled the fretting fatigue life.

Hoppermann and Kordt (2002) reported an interesting finding regarding the benefit of texturing only one or both of the seal mating faces. According to this paper, texturing of just one surface reduced the friction by 40% compared to the standard nontextured case. On the other hand texturing of both mating surfaces increased the friction by 100% compared to the standard nontextured case.

Pride et al. (2002) demonstrated the potential positive effect of micro-surface texturing on reducing breakaway torque and blister formation in carbon–graphite mechanical seal faces.

LST advantages are not limited to liquid lubrication only, and dry gas seals can benefit from LST as well. The main difference is the optimum dimple depth over diameter ratio, which in gas application is much smaller than in liquid application.

Ryk and Etsion (2002) found good agreement with experimental results. In addition it was found that optimum LST is beneficial under starvation as well, where the dimples serve as micro-reservoirs for lubricant. In this study, full LST applied to specimens simulating piston rings, where the conditions were varied from full to starved lubrication

by controlling the lubricant flow rate to the sliding contact. This was done by drip lubrication while varying the time between successive drops. The results show the benefits of LST in reducing friction in both full and starved lubrication conditions.

Etsion and Halperin (2004) also evaluated the idea of partial-LST experimentally, to enhance performance of the parallel thrust bearing. The performance of both unidirectional and bidirectional partial-LST bearings in terms of clearance and friction coefficient was compared with that of a baseline untextured bearing over a load range in which the theoretical model is valid. Consequently the friction coefficient of the partial-LST bearings is much lower, representing more than 50% reduction in friction compared to the untextured bearing. The lower friction make the partial-LST simple parallel thrust bearing concept much more reliable and efficient especially in seal-less pumps and similar applications where the process fluid, which is often a poor lubricant, is the only available lubricant for the bearings.

Brizmer and Etsion (2003) developed a model of a textured parallel slider and analyzed the effect of surface texturing on load carrying capacity. With this study, the potential of laser surface texturing in the form of regular micro-dimples for providing load carrying capacity with parallel thrust bearings was demonstrated. The optimum parameters of the dimples were found in order to obtain maximum load carrying capacity. According to this paper, the micro-dimple “individual effect”, which corresponds to full width texturing, is not useful for developing the large load carrying capacity expected from a hydrodynamic thrust bearing. It can, however, be beneficial in very short slider bearings as is the case with mechanical seals. The micro-dimple "collective effect", which corresponds to partial width texturing, is capable of generating substantial load carrying capacity, approaching that of optimum conventional thrust bearings.

Kobatake and Kawakubo (2003) focused on Laplace pressure in the liquid bridge which are formed when the friction between flat head and disk surfaces become larger. Thus, they studied Laplace pressure of perfluoropolyether lubricant on carbon coated thin-film disk surface in order to increase the recording density of hard disk drives. First, they measured Laplace pressure between transparent flat pins and carbon coated thin-film disks with laser texturing. Using laser textured disks, they could control the distance

between two surfaces precisely by the bump height. The friction coefficient between the pin and the disk surfaces was determined when the interface was fully wet by liquids hence they were able to calculate Laplace pressure of perfluoropolyether lubricant. The Laplace pressure was then calculated using the friction force and liquid wet area when the interface was partially wet by a liquid. The liquid wet area was measured by the observation of the contact point through the transparent pins. The results, which agreed well with calculated curves.

Kovalchenko and Ajayi (2004) carried out a fundamental research work at Argonne National Laboratory in the USA. The effect of LST on the transition from boundary to hydrodynamic lubrication regime was experimentally investigated by measuring friction and electrical-contact resistance in a pin-on-disk unidirectional sliding conformal contact. LST was observed to expand the range of the hydrodynamic lubrication regime in terms of load and sliding speed. Furthermore, LST was observed to reduce the friction coefficient substantially under similar operating conditions when compared with untextured surfaces.

Erdemir and Ajayi (2004) evaluated the potential usefulness of a laser surface texturing or dimpling technology for engine and drive-train applications. This technology produces shallow dimples (typically 4-10 μm deep) 70 to 100 μm in diameter on metallic or ceramic surfaces. Using such surfaces under mixed or hydrodynamic regimes of lubricated contacts provided substantial reductions in friction and wear. The major goal of the project was production and further optimization of such dimples on sliding and rotating contact surfaces of critical engine parts and components to reduce friction and wear. Three different samples (polished, ground, and dimpled) that were used in a series of sliding tests in a unidirectionally sliding wear test machine. These samples were rubbed against both spherical balls (≈ 10 mm in diameter) and flat-ended pins under lubricated sliding conditions. The results showed that under both contact configurations, a dimpled surface provided the lowest friction (especially against the flat-ended pin). However, the friction coefficient of dimpled surfaces was much higher than when they were rubbed against the spherical ball. This may have been due to the relatively high contact pressures that can be generated under such point contact situations. Moreover it is summarized that, highly polished surfaces of ball and flat samples become very rough

as a result of wear under the severe contact pressures of point contact sliding condition, and the friction remains high. For the laser-dimpled surface, friction is high initially but decreases steadily during successive sliding passes and eventually reaches a value of 0.05. The contact surfaces of steel balls wear out and become highly polished. It can be said that substantial reduction in friction during sliding has occurred due to ball wear and hence an increasingly conformal contact between ball and dimpled flat.

McNikel and Etsion (2004) demonstrated the benefit of LST in a dry gas seal application having tests at 12,000 rpm with increasing unit loads to compare the performance of LST seal with that of a nontextured baseline seal. A substantial reduction in friction torque and face temperature was obtained with the LST seal as well as more stable operation compared to the nontextured seal.

Golloch and Merker (2004) presented the use of laser texturing in the form of micro-grooves on cylinder liners of internal combustion engines at the 14th International Colloquium Tribology in Esslingen and showed that this technique provides lower fuel consumption and wear. It is called “laser honing” and now commercially available from the Gehrung Company in Germany.

Hydrodynamic thrust bearings are usually found in magnetic drive seal-less pumps where the process fluid serves as the lubricant for the pump bearings.

Ryk and Kligerman (2005) carried out three series of tests to study the benefit of partial LST in friction reduction of the textured specimens. The first of them consists of untextured specimens to establish a reference, the second utilized full LST specimens for comparison, and the third was performed with partial LST specimens. In all three cases, the increase of average friction with speed and load is observed. It is found that the LST has a substantial effect on friction reduction compared to the untextured reference case. Additional reduction in friction is obtained with partial LST over that of the full LST case. This additional reduction varied depending on the load and speed. The maximum benefit of the partial LST was obtained with the combination of lowest speed and highest load. Some preliminary tests were also performed with production piston rings and cylinder liner segments. The tested piston rings had a cross-section of the “barrel” shape of their face rather than a “cylindrical”- shaped face. According to the results, the

friction in reduction with barrel-shaped rings was much less than with the flat specimen. Some real engine tests that were performed with partial LST barrel-shaped rings also showed very little friction reduction at low speeds. It is demonstrated that barrel-shape is not a good candidate for partial LST. The crowing of the ring face by itself provides a strong hydrodynamic effect that masks the weaker hydrodynamic effect of the surface texturing, especially at high speeds.

Mourier et al. (2006) analyzed the transient lubrication phenomena induced by isolated circular micro-cavities passing through an EHL point contact. By means of an EHL tribometer, a 52100 steel ball, which was micro machined using a femtosecond pulse laser, was tested. It was showed that the micro-cavities do not significantly affect the oil film thickness under pure rolling conditions both experimentally and numerically. They also found that deep micro-cavities induce an oil film decrease on the contrary a shallow micro-cavity locally generates a large increase in the film thickness. The propagation of the oil film reinforcement velocity is found to be increasing when the ball surface is the slowest. In this case, it was established that the local lubricant film reinforcement requires a large viscosity increase inside the micro-cavity. The highly viscous oil volume is moved out of the micro-cavity under the effect of the sliding, and elastically deforms the contacting surfaces.

1.5.2 Theoretical Studies on Laser Surface Texturing

Kligerman and Etsion (2001) developed a finite element model for a laser surface textured circumferential gas seal with micro pores, which are distributed uniformly on one of the annular surfaces, of spherical segment shape and evaluated the hydrodynamic effect of the surface texturing on the seal force balance. They found that the presence of the micro pores on one of the seal mating faces generates substantial hydrodynamic effect that maintains a small clearance between the rotating shaft and the stationary seal ring. This small clearance and the added radial stiffness of the gas film prevent rubbing of the ring against the shaft and hence, may reduce the seal friction and wear. They presented optimized texturing parameters for a typical circumferential gas seal in order to achieve maximum hydrodynamic effect through a parametric investigation and a numerical example.

Ronen et al. (2001) examined the piston-cylinder system with laser surface textured (LST) piston rings. The authors studied the potential use of piston ring micro-surface structure in the form of spherical segment micro dimples to reduce the friction between rings and cylinder liner where the entire ring surface in contact with the cylinder liner was textured. It was demonstrated that significant hydrodynamic effects can be generated by surface texturing even with nominally parallel mating surfaces. The time variation of the clearance between the piston ring and cylinder liner and the friction force at any given operating conditions were obtained by simultaneously solving the Reynolds equation and a dynamic equation. The main parameters of the problem were identified. These were the area density of the dimples, dimple diameter, and dimple depth. An optimum value of the microdimple depth over diameter ratio was found, which yields a minimum friction force. It was found that a friction reduction of 30% and even more is feasible with textured surfaces.

Brizmer and Kligerman (2003) found that, partial LST can improve substantially the load carrying capacity of these simple bearings and make them comparable to more sophisticated tapered or stepped sliders. The textured portion of the slider provides an effective larger clearance than the non-textured portion and hence, the slider is acting as a stepped slider. Test results in water at 1500 and 3000 rpm showed that the textured bearing operated with a clearance that is about 3 times larger and friction that is about 3 times smaller than the case of the nontextured bearing throughout the range of tested loads.

Wang and Zhu (2004) studied the effects of design factors such as dimple size, depth and density on mixed lubrication performance of textured surfaces and showed results about design factors, operating conditions and interface status. According to their study authors found that, at very small dimple sizes film thickness reduced with the increase of dimple size, but this trend turned back when the dimple size further increased. Furthermore the investigation of the second design factor, which is dimple depth, showed that deeper dents yield more severe hydrodynamic reduction and contact ratio increases with depth and for dimple density investigation, it is found that 5% dimple density looks to be the best choice. According to this study the authors claimed that

surface topography and textures play a significant role and the micro geometry must be taken into account.

Siripuram and Stephens [20] developed a theoretical model in order to investigate the effect of deterministic asperity geometry on friction, leakage and film thickness for a given set of operating condition. Predominantly authors were interested in asperity shape, orientation, size and distribution. Authors worked on seven different asperity geometries in both positive and negative configurations. As a result of this study authors found that friction coefficient is largely independent of asperity shape and orientation but very sensitive to asperity area fraction. Also it is found that leakage and film thickness are dependent on asperity shape, concavity, orientation and size.

Kligerman and Etsion (2005) have developed an analytical model to study the potential use of partial laser surface texturing (LST) for reducing the friction between a piston ring and cylinder liner. The advantage of the partial texturing over the full texturing in view of minimizing friction losses was demonstrated. The effect of texturing parameters on the average friction force between a piston ring and a cylinder liner was analyzed for a wide range of ring width and operating conditions. According to their results, an optimum value of textured portion and dimple depth should be selected for a wide range of ring width and operating conditions. The average friction force was not affected by the dimple diameter and it decreased monotonically with increasing dimple area density. It was asserted that, a significant difference between the influence of the ring width and operating conditions on the average friction force in the partial texturing case and in the full texturing case. Furthermore, it was also demonstrated that, the minimum average friction force for the optimum partially textured piston ring is significantly lower than that for the corresponding optimum fully textured ring.

Feldman and Kligerman (2006) investigated the potential of partial laser surface texturing for enhanced tribological performance of hydrostatic gas seals, numerically. A detailed parametric analysis was performed in order to find the optimum laser texturing parameters for maximum seal efficiency. They found that, the performance of a partial LST hydrostatic gas seal is mainly dependent on the dimples area density, and is not affected by the dimple diameter. According to their results, the highest load capacity is

associated with high area density. They demonstrated the actual depth of the dimples has very little effect on the performance of a partial LST seal and added that the dimple depth which is from five to ten times the nominal seal clearance is sufficient. An optimum textured portion value is determined that provides maximum load capacity over a wide range of LST parameters and operating conditions.

1.6 Objective

Engine lube oil consumption has to be taken into consideration as a significant subject due to its effects on engine and catalyst performance, engine oil change intervals and emissions. Lube oil consumption is a severe problem in the development process of modern heavy duty diesel engines. In order to control the amount of engine oil consumption, an accurate, fast, repeatable, and efficient means of measuring oil consumption is required.

The objective of this thesis was to compare the oil consumption measurement of two separate cylinder sets of a modified diesel engine employing a real-time sulfur tracing method by means of a quadrupole mass spectrometer. For this purpose, 9 liter heavy-duty diesel engine with first three cylinders (Cylinder 1-3) having standard plateau honing pattern and last three cylinders (Cylinder 4-6) laser honing pattern was utilized in order to achieve fast and accurate oil consumption measurements. By designing a special sampling system, oil consumption measurements of separate cylinder groups were obtained sequentially under identical running conditions. Investigation of cylinder bore laser surface texturing effects on the lube oil consumption has been accomplished by the developed method without changing the operating conditions of the engine.

2. EXPERIMENTAL METHOD

In this chapter of the thesis, the system requirements, test instrumentation and the development of special sampling system are explained. Furthermore measurement principle and oil consumption calculation take place. Finally, test matrix is represented in the end of the chapter.

2.1 Instrumentation of Measurement System and Test Requirements

The system requirements including high S content lubricating oil, low S content fuel, sensitive SO₂ analyzer and oxidation furnace which are used in order to achieve the real time oil consumption measurement based on S tracer method of test engine is described in this section.

2.1.1 Experimental Setup

The experimental setup was arranged considering the tools and devices of exhaust gas sampling system in order to obtain fast and accurate results by means of the quadrupole mass spectrometer using sulfur tracer method. In the figure 2.1, the configuration of experimental setup is illustrated.

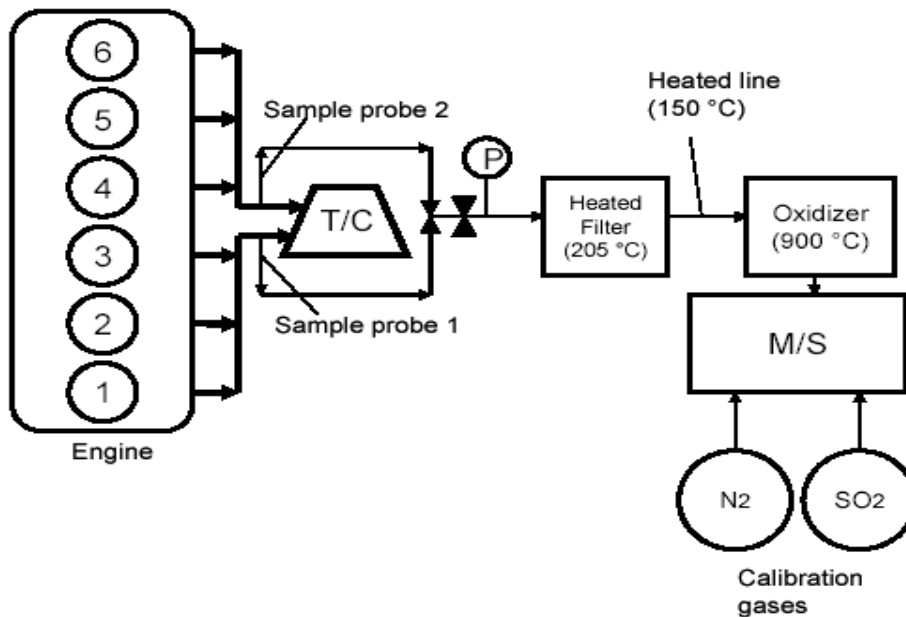


Figure 2.1 Schematic Exhaust Gas Sampling System

The configuration was designed considering the technical problems faced during the experiments. Alternative solutions based on addition of supplementary experimental tools were utilized for troubleshooting.

In exhaust gas sampling system, two exhaust manifolds were separately connected to the first and last three cylinders in order to obtain the sample gas from different cylinder groups regarding the sequence of the test matrix for each test point. Exhaust flow of the two manifolds joined in the turbine of the turbocharger. Exhaust gas samples were collected by means of two separate probes connected to the outlet of the exhaust manifolds. Sample probes were inserted into the exhaust manifold as illustrated in the figure 2.2. A two way valve was employed in order to collect exhaust gas samples from each manifold sequentially under identical running conditions. Therefore, lube oil consumption of separate cylinder groups could be monitored without disturbing the engine steady state operation.

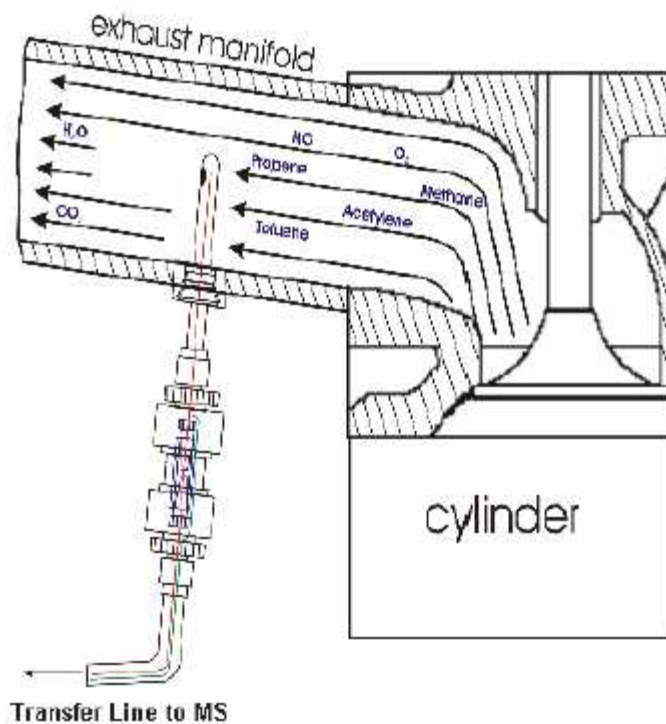


Figure 2.2 Schematic of Sample Probe Mounting

A pressure valve was used to regulate the sample gas flow and pressure to a predetermined value. A 205 °C heated filter was used to trap particulates. Moreover, an oxidation furnace was utilized to convert all sulfur components (SO_3 , SO_4 and H_2S etc.) to SO_2 at high temperature (900 °C). In order to prevent condensation and sulfur loss, an isolated heated line which was approximately 5 meter long and maintained at 150 °C, was used to transfer the exhaust gas sample to oxidation furnace and mass spectrometer. High pressure in the exhaust manifold prior to the turbocharger increases the gas flow and reduces the converter efficiency. Thus, pressure in the sample line was monitored by means of a pressure sensor and adjusts to a predetermined value of 300 mbar relative pressure for each point of the test matrix. A V&F Twin MS mass spectrometer was used to measure the SO_2 concentration in the exhaust stream.

A computer data acquisition system was used in order to record the output of SO_2 and several other engine operation variables. This system includes numerous voltage outputs from the mass spectrometer and engine testing cell. SO_2 concentration of the exhaust stream, air flow, fuel flow, engine torque and power and other temperature and pressure

voltage signals were the output of the system. The signals were input into a computer data acquisition system using the HORUS software. During the experiment, the data collection was saved into a disk for 60 seconds for each test point of the test matrix.

2.1.2 Test Lubricating Oil

Test lubricating oil is an important system requirement since its S content is one of the SO₂ source in the exhaust gas. Therefore, determination of S concentration from lube oil becomes critically important. Only S concentration is naturally present was used as tracer material and no additional tracer material was used that may affect the engine lubrication. Both S contents of lubricating oil and test fuel directly affect the real time oil consumption measurement. Thus, engine is supposed to be operated with high S content lubricating oil in order to provide the lube oil the major source for SO₂ in the exhaust gas.

Since the lubricating oil must provide several criteria depending on the principles of S tracer method, appropriate lubricating oil must be selected according to its qualifications. Firstly, the lubricating oil must have proper viscosity, volatility and formulation so that it will not affect the lube oil consumption results. Furthermore, S concentration must not change the tribological features of the oil and must have a stable concentration over the test period. Colvin et al. (1992) stated that the lubricating oil having higher amount of S content has undesirable effects on engine such as increase of engine wear. Moreover, Ariga et al. (1992) declared that inappropriate S distillation characteristics may cause false measurement results of the oil consumption since sulfur containing materials may vaporize even though lube oil is not consumed. Therefore, to depend on the results obtained during test period in such a case will be misleading.

During the tests, commercially available 15W40, 11720 ppm high S content engine lube oil was used. All analysis on S content of the engine lube oil was performed at Ford Otosan A.S. Laboratories. Additionally, the report for the analysis on S content of test engine is presented in Appendix A.

2.1.3 Test Fuel

SO₂ determined in the exhaust gas is calculated considering S content of both test fuel and lubricating oil. Therefore it is necessary to reduce S contribution of test fuel (Colvin et al., 1992). On the other hand S concentration of a typical diesel fuel is in the range of 50-7000 ppm which has drastically higher S content than the lubricating oil in such case.

Hence, a special order 0.3 ppm diesel fuel was used during the experiments in order to use S content of the lubricating oil effectively and obtain accurate oil consumption results. The report for the analysis on S content of low sulfur test fuel is also presented and it is shown in Appendix B.

2.1.4 Mass Spectrometer

V&F Twin-MS mass spectrometer was used in this study in order to quantify SO₂ concentration of the exhaust stream. In this section the basic principle of mass spectrometer is presented.

Mass spectrometer is utilized for the detection and analysis of ion mixtures of components in order to obtain exact mass determination by differing their mass identically. Separation of matter according to atomic and molecular mass is the basic principle of mass spectrometer. Weighing molecules is the basic operation of mass spectrometry. For this reason, mass spectrometer is based on the separation of charged particles moving in an electrical or magnetic field according to their mass/charge ratio (m/z) (Hoffman and Stroobant, 2001).

The mass spectrometer consists of four basic components which are standard in all mass spectrometers. As illustrated in figure 2.3, sample inlet, an ionization source, a mass analyzer and an ion detector are the major components of the mass spectrometer. The sample inlet and the ionization source are combined in some instruments whereas others combine the mass analyzer and the detector. All sample molecules undergo the same processes apart from the instrument configuration. Sample inlet is the component which provides the entrance of sample molecules into the instrument through a sample inlet. Subsequently the sample molecules are converted to ions in the ionization source in order to pass through the mass analyzer. In the mass analyzer, the ions are separated

according to their mass/charge ratio composing the data about the molecular weight of the compound and its chemical structure. The ions are directed into the ion detector after they are separated by the mass analyzer. The detector is employed in order to convert the ion energy into electrical signals which are then transmitted to a computer (A History of Mass Spectrometry, 2005).

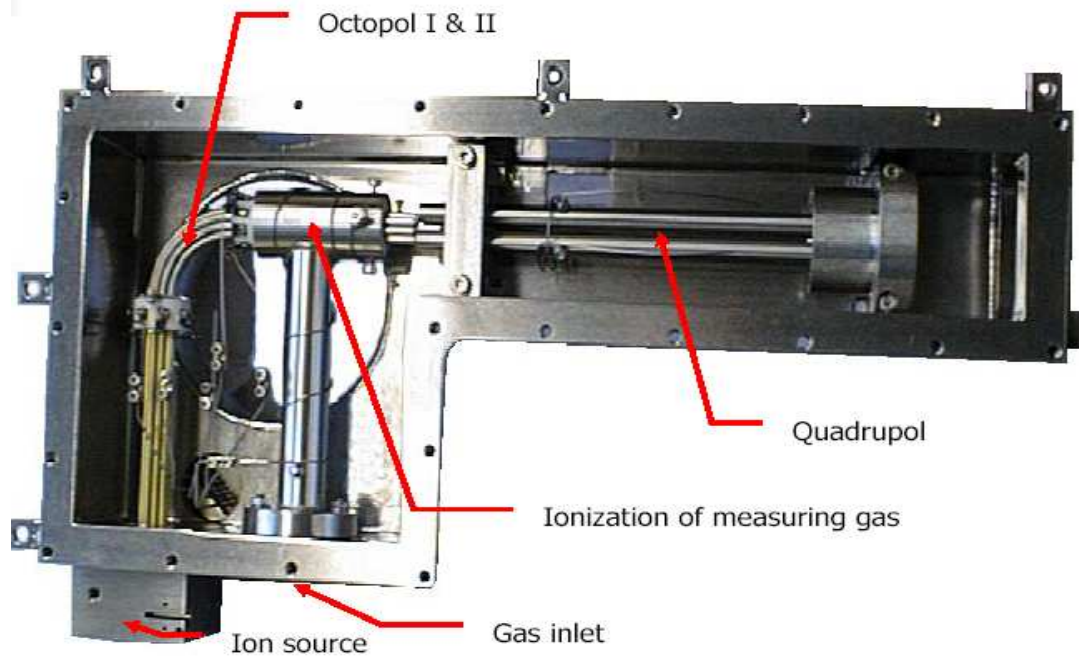


Figure 2.3 Basic Components of Mass Spectrometer

2.1.4.1 The V&F Twin MS Technology and Instrumentation

During the tests of this study, Twin MS type mass spectrometer was employed for the detection of SO₂ concentration in the exhaust stream. In this section the technology and the instrumentation of mass spectrometry is described.

Consequential developments within the range of analytical equipment offer room for improvements within processes and catalytical reactions which then lead towards state of the art engines.

The Twin MS dual mass spectrometer, illustrated in the figure 2.4, features a unique combination which has been specifically developed in order to measure pre- and post catalyst fast and simultaneously. The single robust platform consists of two parallel

installed Ion Molecule Reaction (IMR) mass spectrometers, each configured with a single heated sample inlet port.



Figure 2.4 V&F Twin MS

Targeting the specific needs within the wide range of applications, the series Twin MS is based on two identical, parallel installed IMR mass spectrometer in one single housing. IMR technique offers a fast, selective and interference free measurement. The technique also enables high selectivity and large measurement range. The separation of ions with identical masses is the basic principle of the technique. The interpretation of the detected results can not be confused by fragmentation or overlapping spectra.

IMR means using primary ions with lower energy level between 10 eV and 14 eV to completely ionize the probe gas molecules. The signal noise ratio will be optimized by the integrated octopole separator, focusing the primary ions and filtering out any interferences. The quadrupole mass filter which is illustrated in the figure 2.5, consists of four parallel metal rods arranged in parallel. The rods have opposing or out-of-phase time-varying (AC) voltages. These voltages affect the trajectory of ions traveling

between the four rods. For given a given set of voltages, only ions of a certain mass-to-charge ratio pass through the quadrupole filter and all other ions are thrown out of their original path. A mass spectrum is obtained by monitoring the ions passing through the quadrupole filter as the voltages on the rods are varied. Quadrupole filters reduce the background noise and generally improve the precision of mass measurements.

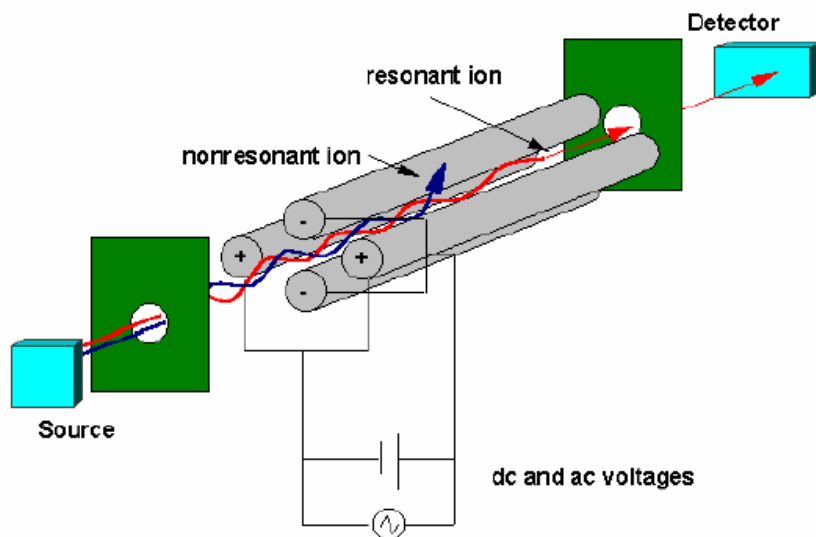


Figure 2.5 Quadrupole Mass Filter

The two separate sample gas inlets (with temperature and pressure compensation) offer to measure two identified molecules at each of the sample streams at once (pre and post catalyst analysis). Both inlets are designed to avoid any discrimination of the gas and minimize the contamination due to condensation or particulate matters. A single and easy to use software package combines both analyzers in terms of all system's set-up and data reporting issues. A schematic structure of mass spectrometer is illustrated in the figure 2.6.

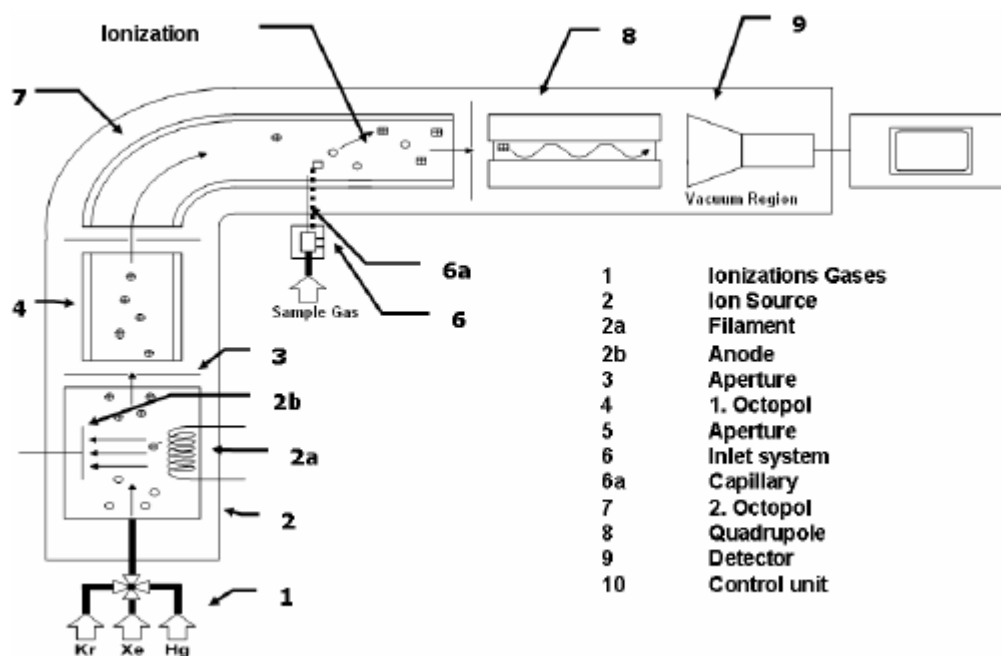


Figure 2.6 Schematic Structure of V&F Twin MS

The detection principle of mass spectrometer is based on the analysis of the molecular weight of the substances. Sample gas is introduced to a high vacuum chamber and transformed into ions that are subsequently mass selected by electromagnetic fields and counted in a particle detector. Since different molecules may carry the identical molecular weight, the instrument uses different ionization levels to distinguish between mass identical molecules. Every molecule has an individual energy that is necessary to remove an electron and thus convert the molecule into an ion. The Twin-MS provides the operator the option of choosing mercury (Hg), xenon (Xe), or krypton (Kr) as the ionization source gas that decreases the possibility of interferences from isobaric molecules. Indeed, the ionization potential of Hg ions is 10.54 eV, of Xe ions is 12-13 eV, and of Kr ions is 14 eV. A Kr ion beam with 13.9 eV energy, for instance, separates the mass identical molecules N₂ (14.2 eV) and CO (13.7 eV). The source filament emits electrons with energy of 20-25 eV. The ionization source gas is passed over the source filament where it is ionized by electron impact ionization. A several microampere ionization source gas beam is formed and guided to a high frequency first part of the octopole, where it is focused. This beam is accelerated in the octopole via a direct current.

The sample gas enters the second octopole at the midpoint of its length and mixes with the ionization source gas. The portion of the sample gas that has an ionization potential lower than that of the ionization source gas is ionized to parent ions and is accelerated in the second part of the octopole. Sample gas then passes through a 200 mm quadrupole rod where the ion of choice is focused on the basis of its mass-to-charge ratio and afterwards passed on to a detector (electron multiplier detector) (Laroo, 2002). Finally, detector converts the ion energy into electrical signal, which are then transmitted to computer. The technical specification of V&F Twin MS is given in Table 2.1.

Table 2.1 Technical Specification and Rating Data of V&F Twin MS

Mass Range	0 -500 amu
Mass Resolution	< 1 amu
Measurement Time	1 - 6500 msec/amu
Measurement Range	10 ⁴
Response Time	T 90 < 30 msec
Source Gas Switching Time	< 250 msec
Detection Limit	10 ppb i.e. benzene (optional: 1 ppb)
Drift	<± 5% per 12 hrs at 1 ppm benzene
Reproducibility	<± 3% at 1 ppm benzene
Accuracy	<± 2% at 1 ppm benzene
Environmental Temperature	20-35°C with 1°C/h maximum temperature variation
Environmental Humidity	Max. 80% (none condensation)
Gas Consumption	30 – 250 ml/min
Main Power	220 V / 50 Hz, 1250W (optional: 110 V / 60 Hz)
Dimensions	590 x 650 x 1000 mm
Weight	125 kg

2.1.5 Oxidation Furnace

A Measurement Technologies Model 1000 type thermal oxidizer was utilized to convert all S components to SO₂ at high temperature (900 °C) during all tests. The operation principle of the thermal oxidizer is to convert any S containing material such as SO₃, SO₄, and H₂S in the exhaust sample to SO₂. If the S content both in fuel and lubricating oil do not completely form SO₂ during combustion in S tracer method, then the experimental error occurs (Hanaoka et al., 1979). Moreover, Ariga et al. (1992) underlined that 98% of S is converted to SO₂. Additionally, Villinger et al. (1993) asserted that in combustion conditions with λ less than 0.9 the reducing atmosphere of

the engine's exhaust gas contains enough hydrogen, carbon monoxide and unsaturated hydrocarbon residuals to convert the sulfur into gaseous sulfur emissions.

2.1.6 Heated Line

In order to prevent condensation and sulfur loss, an isolated heated line, maintained at 150 °C, was used to transfer the exhaust gas sample to oxidation furnace and mass spectrometer. When the exhaust gas starts to be cooled in transfer period to mass spectrometer, moisture condenses inside the transfer line. Therefore moisture may combine with sulfur causing the formation of sulfuric acid (H₂SO₄). Hence, the temperature of the sample line must be greater than 100 °C for the prevention of sulfur loss (Hanaoka et al., 1979).

2.1.7 Test Engine Specification

Test engine used in the experiments was a prototype of newly design 9 liter, direct injection and turbo-charged FORD ECOTORQ heavy duty diesel engine. Final power cylinder components, surface texture and calibration and thus the measured data do not represent the commercially available engine. The specifications of the test engine are listed in the Table 2.2.

Table 2.2 Test Engine Specifications

Engine Configuration	6 Cylinder in-line
Fuel Injection System	Common Rail DI Diesel (1800 bar)
Scavenging System	Turbo-Charged, Inter-Cooled
Bore	115 mm
Stroke	144 mm
Swept Volume	8.974 L
Peak firing pressure	190 bar
Rated power	295 kW @ 2200 rpm
Peak torque	1600 Nm @ 1200 rpm
Max. Operational Speed	2200 rpm
Max. Continuous Over Speed	3100 rpm
Valve Train	OHV (Overhead Valve), 4 valves per cylinder

Test engine is significant with its design which provides the evaluation of laser surface texturing effects on lube oil consumption. Test engine was a modified engine with first

three cylinders (Cylinder 1-3) having standard plateau honing pattern and last three cylinders (Cylinder 4-6) having laser honing pattern.

The blocks of the engine were honed at Gehring GmbH & Co KG. Basing on the structuring process in cylinder working surfaces in internal combustion engines honing machine was used for the basic set up of machining. Laser head was connected to spindle in order to enable rotation and lift movements. A Q-switch Nd YAG laser was used as a laser beam source, for laser structuring process. Complete ablation of the material was achieved by the intensities of the focus plane.

It was preferred to use a laser machining process to produce the pockets and secondary pockets in an otherwise smooth surface. This was because such a laser machining process allows each pocket to be accurately produced and also the use of laser machining permits considerable flexibility in the location size, shape and orientation of the pockets. However, it would be appreciated that alternative fine honing and/or pocket machining methods such as electron beam or other suitable mechanical honing methods could be used instead of the laser honing method.

Two different configurations were applied at upper and lower sides of the laser-honed cylinder liners. At upper side of the cylinder liner, each pocket had a length of approximately 3 mm. The pockets were spaced around the cylinder bore wall approximately 1 mm apart from each other in horizontal directions and 2 mm apart from each other in vertical directions. On the other hand, at lower side of the cylinder liner, each pocket had a length of approximately 3mm. Moreover, the pockets were spaced around the cylinder bore wall approximately 2mm apart from each other in horizontal directions and 5 mm apart from each other in vertical directions causing widely set configuration of micro pressure pockets. The schematic of blocks configuration is illustrated in the figure 2.7.

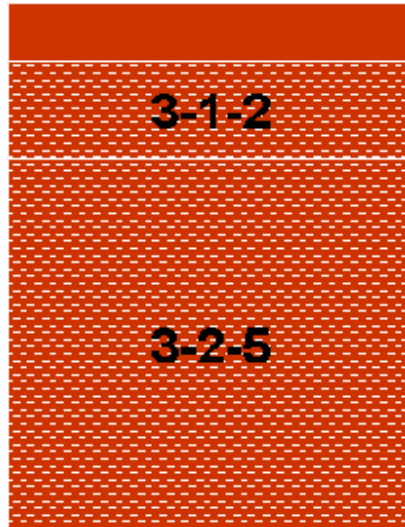


Figure 2.7 The Configuration of the Blocks (Cylinders 4-6)

As the piston approaches its bottom dead center and top dead center positions, the relative velocity of the piston rapidly decreases down to zero at bottom dead center and top dead center. In these regions, the effect of hydrodynamic lubrication also rapidly decreases and the effect of mixed lubrication becomes prevalent. At the region where is adjacent to top dead center, a more frequent configuration of micro pressure pockets was preferred in order to provide an advantageous source of lubrication for the piston rings and to prevent scuffing which is an adhesive-wear event in which two parts slide against each other in a lubricant-starved condition. Scuffing typically happens when the lubricating oil film at the interface is broken. The potential exists for this loss of lubrication due to overheating which causes the lubricating oil film to decompose, excessive force between the parts, or insufficient oil at the interface. Moreover, it is asserted that, the use of pockets rather than grooves reduces the tendency for scuffing and blow-by, a phenomenon which is encouraged by continuous grooves parallel to the axis of the cylinder bore (Engine and A Method of Making Same, 2007). The cylinder bore wall so machined therefore takes advantage of the prevalent lubrication effects at different regions to reduce friction, wear and oil consumption.

2.2 Determination of Oil Consumption Based on Mass Spectrometry

Test procedure for real time oil consumption which permits the measurement of each cylinder group sequentially is detailed in this section. Same process chain and timing are applied to the test system at each test point of the test matrix.

2.2.1 Test Procedure

Since the sulfur content of both test fuel and lube oil are needed for the calculation of oil consumption, the samples including lubricating oil and test fuel were analyzed. The samples were taken both before and after experiments in order to have laboratory analysis on sulfur concentration. The calibration of the mass spectrometer was needed undoubtedly in order to obtain accurate results. The mass spectrometer was calibrated at each value of engine speed varying with load according to the test matrix. Calibration was accomplished with nitrogen gas (N_2) as inert gas and N_2 containing 2% ppm (by volume) SO_2 as span gas. All the processes described up to now take place before the real time oil consumption measurement.

Before collecting data, the engine was operated at idle in order to warm up the oil temperature to approximately 90 °C. After engine warm up period, the engine was set to the first operation point of the test matrix combining both a specific engine speed and load value. The maximum engine speed which is 2200 rpm at full load was the first operation point of the test matrix and the values were decreased subsequently considering the predetermined test points of the test matrix.

The duration of each test cycle was approximately 5 minutes. The first 4 minutes were used for the change of the oil consumption measurement of current cylinder group by means of a two-way valve, the calibration of mass spectrometer and reaching steady-state condition for the current operation point of the test matrix. On the other hand, data recording for the entire measured real time engine operating conditions took place during the last minute with a sampling frequency of 10 Hz. Furthermore, during the test period all the engine conditions and ambient parameters were measured simultaneously. The same procedure was applied completely for each operation point of the test matrix. After the real time oil consumption measurement was completed, the recorded outputs of

the entire measurements including SO₂ concentration of the exhaust stream, air flow, fuel flow, all other engine parameters and ambient conditions were transferred into a spreadsheet. Consequently, the mass of oil consumed was determined using SO₂ concentration of the exhaust stream of the engine, mass of air and fuel through the engine.

2.2.2 Calculation of Oil Consumption

Three assumptions are made in the calculation of oil consumption period. Firstly, sulfur was assumed to be distributed equally in the lubricating oil. Another significant assumption was the stable value of sulfur concentration in the lubricating oil during the test period. Finally, all sulfur components in the sample gas were assumed to be converted to SO₂ in the oxidation furnace.

In order to compare the oil consumption measurements of the cylinder groups having standard plateau honing pattern and laser honing pattern, oil consumption rates of the cylinder groups had to be determined. The calculation of oil consumption in grams per hour (g/h) was accomplished by the formulation combining additional engine and exhaust parameters. Oil consumption was calculated using the amount of sulfur quantities entering and leaving the combustion chamber and other engine parameters recorded by the computer data acquisition system. The flowchart of calculation is illustrated in figure 2.8.

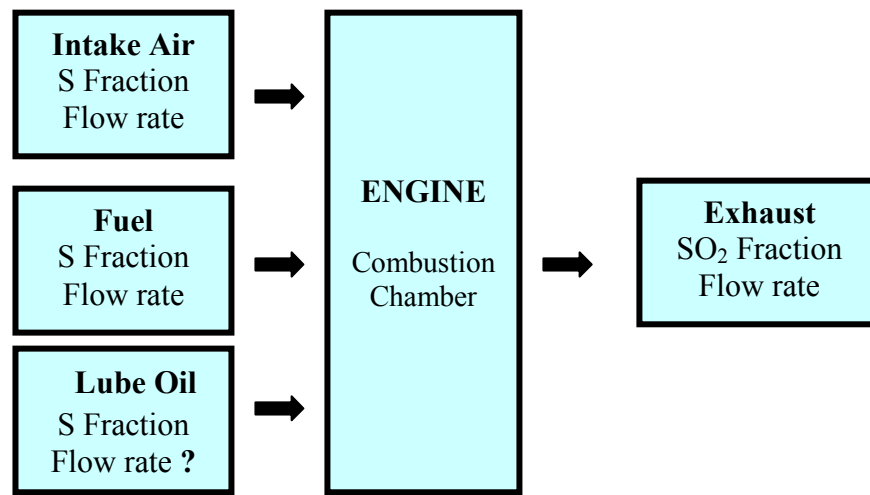


Figure 2.8 Calculation Flowchart

As it is indicated previously, the analysis on sulfur contents of both test fuel and lubricating oil were needed for the calculation of oil consumption. S fraction of air was neglected during the calculations since the SO₂ concentration of the ambient air is very low. Moreover, flow rate of intake air and fuel consumption were measured simultaneously at each operating point of the test matrix during the experiments. Hence, total exhaust stream was calculated with the sum of fuel consumption and intake air flow. Finally, SO₂ concentration of the exhaust gas was calculated by means of the mass spectrometer. Oil consumption rate was determined by subtracting the mass flow of SO₂ contribution of the fuel from the measured SO₂ mass flow in the exhaust. The calculation of oil consumption was circumstantiated as follows:

a) Determining SO₂ mass flow of total exhaust in gram per hour;

$$\dot{m}_E = \dot{m}_A [kg/h] + \dot{m}_F [kg/h] \quad (2.1a)$$

$$\dot{n}_E = \frac{\dot{m}_E [kg/h] 1000}{M_E [g/mol]} \quad (2.1b)$$

$$\dot{m}_{SO_2,E} = \dot{n}_E [mol/h] M_{SO_2} [g/mol] S_{exhaust} [ppm] 10^{-6} \quad (2.1c)$$

where;

\dot{m}_E : Exhaust mass flow

\dot{m}_A : Intake air mass flow

\dot{m}_F : Fuel mass flow

\dot{n}_E : Mol flow of exhaust gas

M_E : Molar mass exhaust

$\dot{m}_{SO_2,E}$: SO₂ mass flow in the exhaust

b) Determining SO₂ mass flow contribution of fuel in the total exhaust in gram per hour;

$$\dot{m}_{S,F} = \dot{m}_F [kg/h] 1000 S_{fuel} [ppm] 10^{-6} \quad (2.2a)$$

The molar mass of S is 32 g/h and SO₂ is 64 g/h, then;

$$\dot{m}_{SO_2,F} = 2 \cdot \dot{m}_{S,F} [g/h] \quad (2.2b)$$

where;

$\dot{m}_{S,F}$: S mass flow contribution of the fuel

S_{fuel} : S concentration in fuel

$\dot{m}_{SO_2,F}$: SO₂ mass flow contribution of fuel

c) Determining SO₂ and S mass flow contribution of the lubricating oil in the total exhaust in gram per hour;

$$\dot{m}_{SO_2,O} = \dot{m}_{SO_2,E} [g/h] - \dot{m}_{SO_2,F} [g/h] \quad (2.3a)$$

$$\dot{m}_{S,O} = \frac{\dot{m}_{SO_2,O} [g/h]}{2} \quad (2.3b)$$

$\dot{m}_{SO_2,O}$: SO₂ mass flow contribution of oil

$\dot{m}_{S,O}$: S mass flow contribution of oil

d) Determining oil mass flow (oil consumption) in gram per hour;

$$\dot{m}_O = \frac{\dot{m}_{S,O} [g/h]}{S_{oil} [ppm] 10^{-6}} \quad (2.4)$$

where;

\dot{m}_O : Oil mass flow

S_{oil} : S concentration of oil

In the last step, oil consumption rate is calculated in gram per hour using the combined formulation below:

$$\dot{m}_{OC} = \left[\frac{32.(\dot{m}_A + \dot{m}_F) \cdot S_{exhaust}}{M_E \cdot S_{oil}} - \frac{\dot{m}_F \cdot S_{fuel}}{S_{oil}} \right] \cdot 1000 \quad (2.5)$$

where;

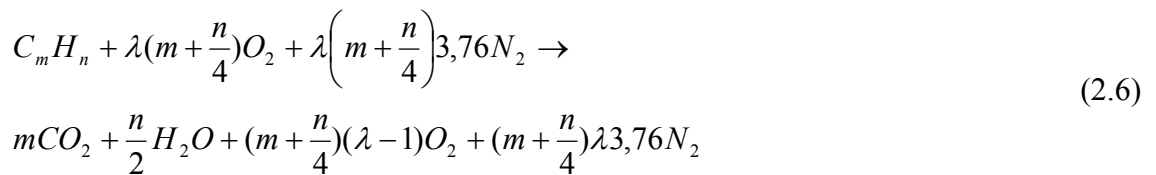
\dot{m}_{OC} : Oil consumption rate

This formulation was used to determine the oil consumption rate using the data recorded into the computer data acquisition system for each operation point of the test matrix. Finally, the results obtained from the formulation were divided by 2 in order to determine the lube oil consumption of each cylinder group.

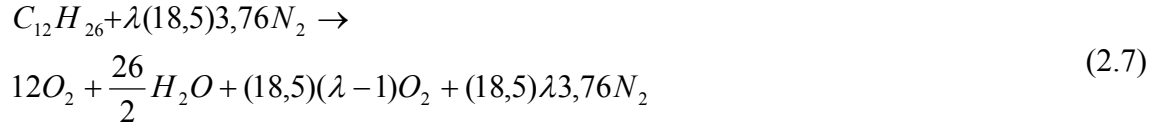
2.2.3 Calculation of Exhaust Molar Mass

Analysis which are conducted by the quadrupole mass spectrometer determines the SO₂ concentration of exhaust gas sample as parts per million (ppm) by volume or parts per billion (ppb). Thus, it is essential to convert the results in ppm by volume into ppm by weight in order to obtain the results of oil consumption in gram per hour. For this purpose molar mass of exhaust (M_E) gas has to be calculated. On the other hand, M_E is not constant, since the air/fuel ratio is not constant for different engine operation points. For this reason M_E was calculated by determining the relative air to fuel ratio using the chemical formula of diesel fuel at each operation point of the test matrix.

The general combustion equation is given below:



where λ is relative air to fuel ratio, and $C_m H_n$ is chemical formula of diesel fuel. The average chemical formula for common diesel fuel is $C_{12}H_{16}$, ranging from approximately $C_{10}H_{22}$ to $C_{15}H_{32}$. Hence the equation becomes:



Total mol number of exhaust which is indicated with N determined by the sum of mol numbers of exhaust products are needed to calculate M_E . Finally M_E is calculated with dividing the total mass of exhaust products by N .

$$N = 12 + 13 + (18,5).(\lambda - 1) + (18,5).\lambda.3,76 \quad (2.8)$$

$$M_E = \frac{1}{N} [12.44 + 13.18 + 18,5.(\lambda - 1).32 + 18,5.\lambda.3,76.28] \quad (2.9)$$

This calculation is used in the oil consumption calculations for each operating point of the test matrix and the average value of M_E was found approximately 28,773 g/mol.

2.2.4 Test Matrix

Test matrix applied in this study, includes 24 test points in order to evaluate the oil consumption of the modified engine having its cylinders with standard plateau honing pattern and laser honing pattern. In Table 2.3, test matrix of each test point is given for both cylinder groups with the related torque and power values.

Table 2.3 Test Matrix

CYLINDERS (1-3)				
rpm	load	Nm	kW	HP
2200	100	1298,826	299,5888	407,324
2200	75	1002,787	231,3254	314,5178
2200	50	658,3495	151,8844	206,5039
2200	25	337,1041	77,7684	105,7338
1600	100	1567,417	263,0297	357,6215
1600	75	1182,188	198,426	269,7838
1600	50	765,1179	128,4149	174,5938
1600	25	388,5601	65,22749	88,68213
1000	100	1123,61	118,0056	160,4358
1000	75	863,911	90,7661	123,4043
1000	50	591,2953	62,14581	84,49346
1000	25	297,9558	31,30619	42,5669
CYLINDERS (4-6)				
rpm	load	Nm	kW	HP
2200	100	1298,826	299,5218	407,2328
2200	75	1002,787	231,4534	314,692
2200	50	658,3495	151,8448	206,4525
2200	25	337,1041	77,79965	105,7775
1600	100	1567,417	263,0264	357,6166
1600	75	1182,188	198,0133	269,2239
1600	50	765,1179	128,4191	174,5998
1600	25	388,5601	65,27469	88,7485
1000	100	1123,61	118,2036	160,7113
1000	75	863,911	90,78348	123,4291
1000	50	591,2953	62,14635	84,49878
1000	25	297,9558	31,31019	42,56839

The test points of the test matrix were selected considering the engine oil consumption characteristic. 2200 rpm was the maximum speed of the engine and it was also the highest value for engine speed in the test matrix. Moreover, 1000 rpm was selected in order to evaluate lube oil consumption of separate cylinder groups at low engine speed conditions. Four different load values including 25%, 50%, 75% and 100% were applied to the modified engine for each engine speed. Finally, comparative graphs were prepared using the values of average torque, power, lube oil consumption and specific oil consumption for each operating point of the test matrix.

3. EXPERIMENTAL RESULTS

3.1 Lube Oil Consumption Results

The results obtained during the real oil consumption measurement tests were utilized in order to evaluate laser surface texturing effects on lube oil consumption and compare to that of reference cylinders which have standard plateau honing pattern. The oil consumption values in gram per hour were calculated during engine operation by using SO₂ concentration of exhaust gas, intake air flow and fuel consumption for each separate cylinder set. Entire measurement data used in the calculations and calculated results are presented with a detailed table in Appendix C and D. The lube oil consumption results of the test engine are shown in Table 3.1. In the Figure 3.1 and Figure 3.2 the lube oil results of two cylinder groups are presented at 25% load and 50% load respectively. These results represent the combined oil consumption of the cylinders.

Table 3.1 Lube Oil Consumption Results

LUBE OIL CONSUMPTION (g/h)								
	25%		50%		75%		100%	
	Cyl.1-3	Cyl.4-6	Cyl.1-3	Cyl.4-6	Cyl.1-3	Cyl.4-6	Cyl.1-3	Cyl.4-6
1000 rpm	2,5025	2,4626	3,0891	2,7564	4,6366	4,5634	5,4662	5,2891
1600 rpm	4,7499	3,9893	7,6878	6,1545	9,4423	9,7938	16,1826	15,7421
2200 rpm	6,5630	5,8514	10,0608	10,4032	14,0372	14,8989	23,0657	20,9578

As seen in both of the figures, lube oil consumption increases with increasing engine speed as a general trend. The lowest value of lube oil consumption was 2.46 g/h and it was obtained from the second cylinder group which has laser honing pattern at 25% load with 1000 rpm. Moreover, there is only a slight difference of lube oil consumption between the cylinder groups having different honing patterns. This effect may be caused due to the cylinder surface texture parameters which will be discussed in detail in the following part in the section.

Same trend with increasing engine speed was also observed with 50% load for lube oil consumption. At 1000 rpm and 1600 rpm the second cylinder group had lower oil consumption than that of the first cylinder group. However, at the highest value of engine speed the oil consumption of laser honed cylinders group was greater. Moreover, the highest value of the difference between oil consumption of separate cylinder groups was obtained at 50% load, 1600 rpm.

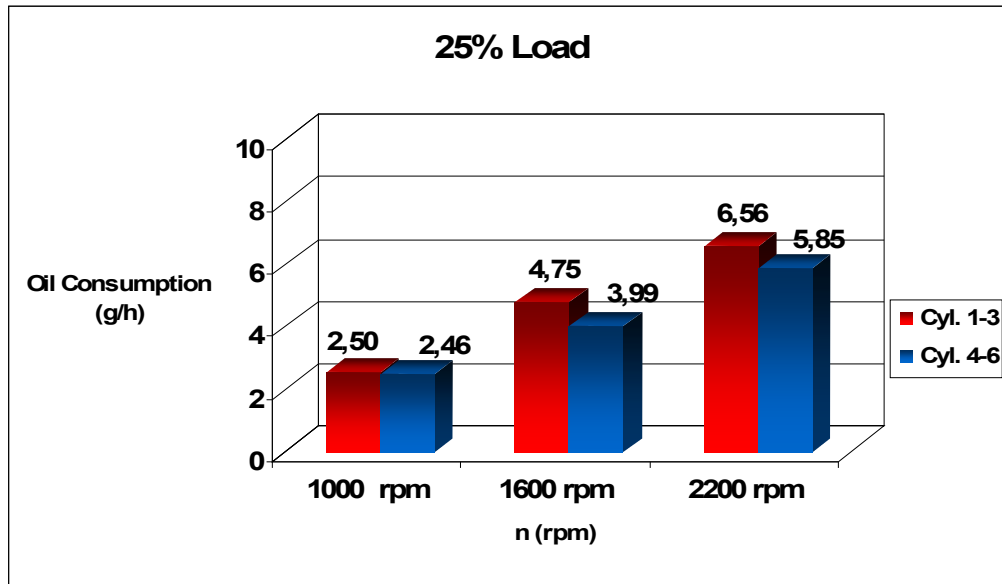


Figure 3.1 Oil Consumption at 25% Load

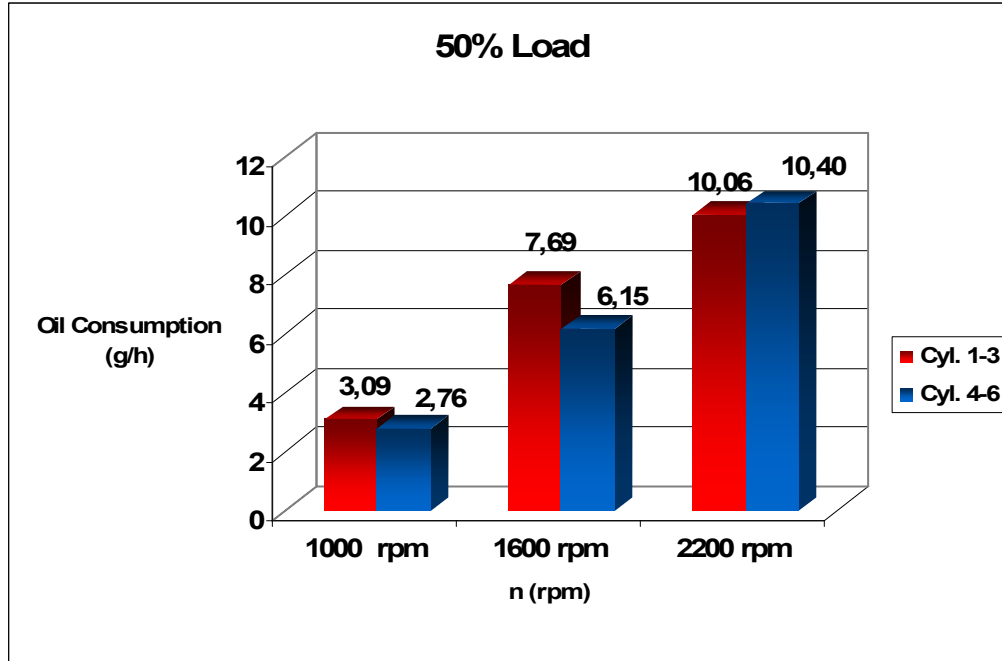


Figure 3.2 Oil Consumption at 50% Load

The lube oil consumption had tendency to increase with increasing speed and load for also 75% load test points as shown in Figure 3.3. At 1000 rpm, the lube oil consumption was only 8% higher for the cylinder group 1-3 with standard plateau honing pattern.

It was observed from the results at 100% load which are presented in Figure 3.4, the highest value of lube oil consumption was 23.07 g/h at 2200 rpm with cylinders 1-3. This effect may be due to increasing speed. Since increasing speed increases the amount of oil transported to combustion chamber surface by means of piston rings. Higher amount of oil is retained within the valleys of the plateau honed surface, therefore the amount of oil exposed to combustion increase with increasing surface roughness. Moreover, the difference of lube oil consumption results between separate cylinder sets reached 2.11 g/h at 2200 rpm. For other engine speeds there is only a slight difference between different cylinder groups.

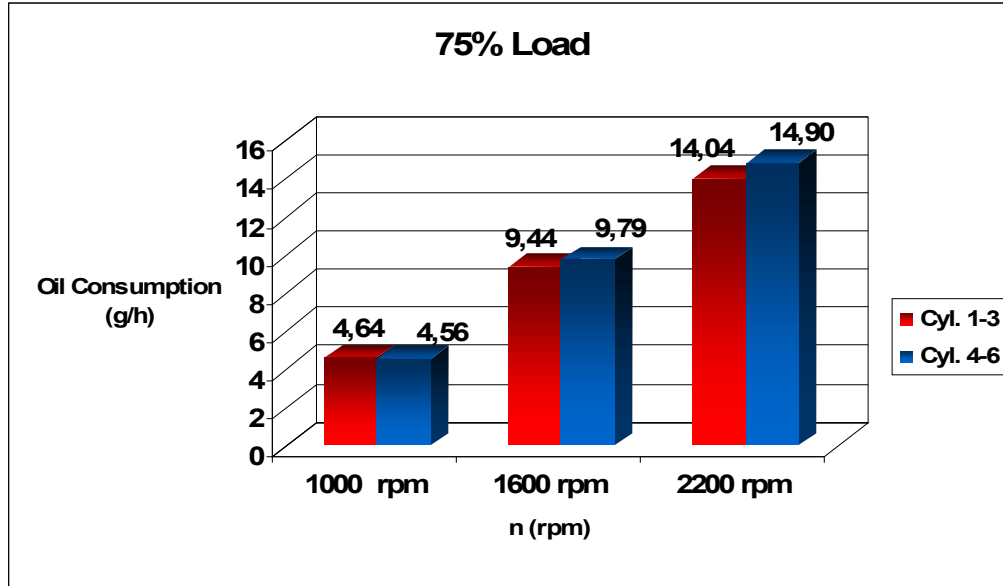


Figure 3.3 Oil Consumption at 75% Load

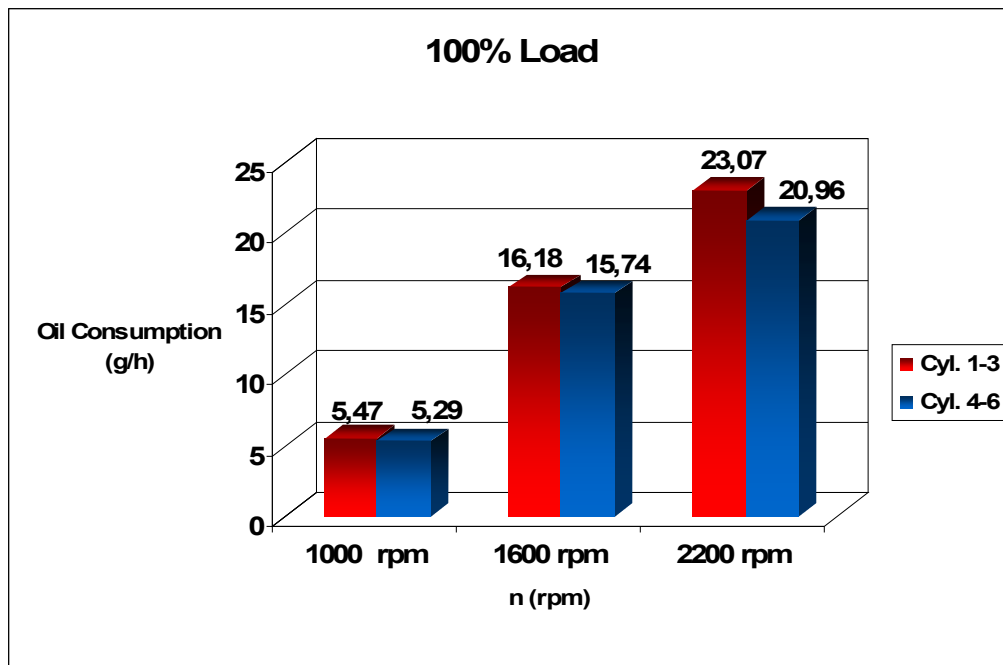


Figure 3.4 Oil Consumption at 100% Load

Figure 3.5 shows that the lube oil consumption has tendency to increase with increasing load. At 1000 rpm the lowest value of oil consumption was obtained at 25% load with laser honed cylinder group. On the other hand, the difference of oil consumption between each separate set was not greater than 0.04 g/h at this point. Moreover, plateau

honed surfaces have minor excess on lube oil consumption at 1000 rpm for each load value.

Figure 3.6 demonstrates that, cylinders 4-6 have higher oil consumption at 1600 rpm for 75% load, which has also showed the same trend in a previous study having two separate cylinder sets with high and low surface roughness (Akalin et al., 2008).

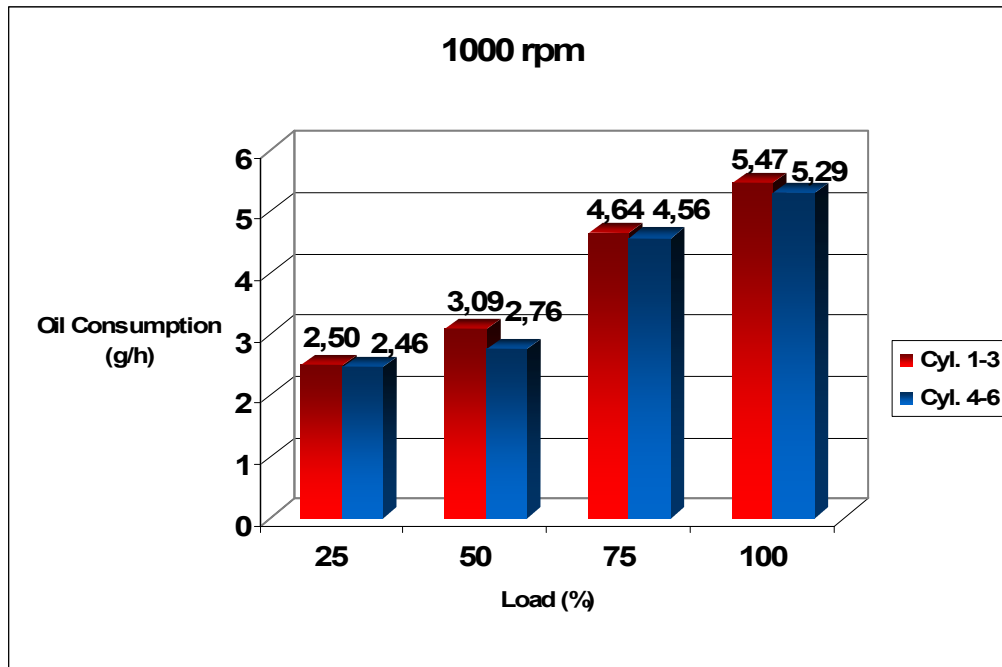


Figure 3.5 Oil Consumption at 1000 rpm

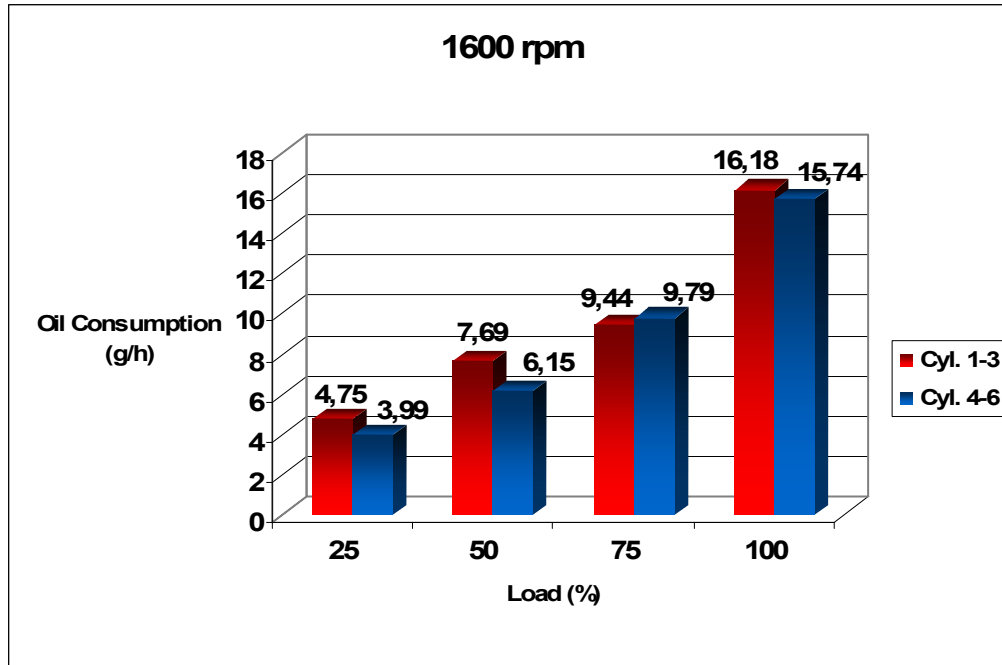


Figure 3.6 Oil Consumption at 1600 rpm

In Figure 3.7, the lube oil consumption shows a general trend with increasing load at 2200 rpm. Moreover, the highest difference between the cylinder groups was observed at 100% load. Since the thermal output of the engine is at peak and evaporation is accelerated, the difference becomes more obvious at full load.

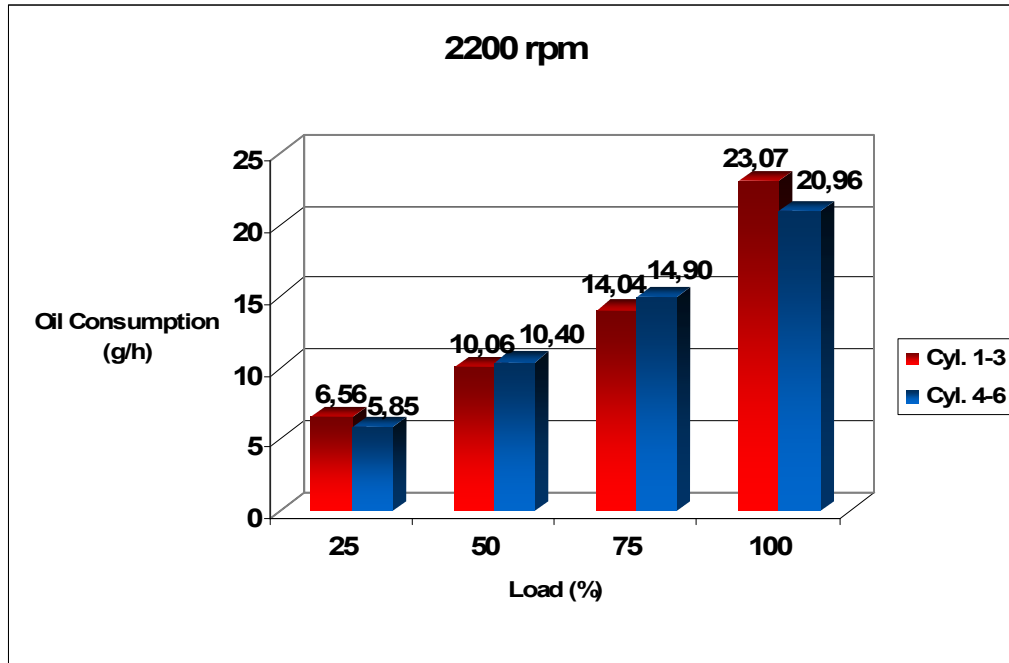


Figure 3.7 Oil Consumption at 2200 Load

The metrological analysis which presents cylinder surface texture parameters of test engine is given in Table 3.2. Since surface roughness parameters may have large variance for various locations along the cylinder bore, the surface roughness parameters for each cylinder bore were calculated averaging the measurements of large number of axial and circumferential locations on cylinder bore surface. These surface roughness parameters were measured prior to a six hours of running-in procedure applied under idle and partial load conditions.

Table 3.2 Cylinder Surface Texture Parameters for Test Engine

CYLINDER	Ra	Rz	Rpk	Rk	Rvk	Mr1	Mr2
1	0,65	4,52	0,38	1,63	1,56	5,75	79,16
2	0,6	4,22	0,35	1,6	1,37	6,74	81,12
3	0,51	3,84	0,31	1,31	1,24	6,53	80,91
Cyl. 1-3	0,59	4,19	0,35	1,51	1,39	6,34	80,40
4	0,22	2,43	0,27	0,43	1,27	13,17	85,51
5	0,25	2,75	0,27	0,5	1,52	12,57	86,93
6	0,19	2,17	0,21	0,34	1,19	14,11	84,88
Cyl. 4-6	0,22	2,45	0,25	0,42	1,33	13,28	85,77

First cylinder group has higher average roughness parameters. Moreover, both of the separate cylinder sets have similar valley material component (Mr_2) and reduced valley depth (Rvk) parameters which are found to be the most effective parameters in determination of “Oil Retaining Volume” (Hill, 2001). As it is observed from the experimental results of oil consumption, there is only a slight difference between the cylinder groups which both have similar oil retaining volume. Hill (2001) asserted that, high levels of Rvk and associated oil retaining volume serve to increase oil flow to the top ring. As a result, oil retaining volume is a critical parameter that should be controlled to minimize oil consumption. In other words, both Ra and Rvk parameters must be decreased in laser honing in order to obtain lower lube oil consumption measurements.

3.2 Specific Oil Consumption Results

The effects of engine power on oil consumption were also investigated. Specific oil consumption results of test matrix are given in Table 3.3.

Table 3.3 Specific Oil Consumption Results

SPECIFIC OIL CONSUMPTION (g/kWh)								
	25%		50%		75%		100%	
	Cyl.1-3	Cyl.4-6	Cyl.1-3	Cyl.4-6	Cyl.1-3	Cyl.4-6	Cyl.1-3	Cyl.4-6
1000rpm	0,1599	0,1573	0,0994	0,0887	0,1022	0,1005	0,0926	0,0895
1600rpm	0,1456	0,1222	0,1197	0,0958	0,0952	0,0989	0,1230	0,1197
2200rpm	0,1688	0,1504	0,1325	0,1370	0,1214	0,1287	0,1540	0,1399

As seen in Figure 3.8, the specific oil consumption results at 1000 rpm have similar characteristic for 50%, 75% and 100% engine load conditions. However, at 25% engine load points where the engine power is low, oil consumption rate in g/kWh is high for both cylinder groups having dissimilar honing pattern. Moreover the lowest specific oil consumption measurement was obtained at 50% load with laser honed cylinder blocks.

In Figure 3.9, similar trend was observed for also the specific oil consumption results at 1600 rpm. Moreover, the difference of oil consumption rate in g/kWh between each cylinder group was greater at 25% and 50% engine load. On the other hand, at 75% load

and 100% load, there is not a significant difference for specific oil consumption between two cylinder groups. In addition to this, the specific oil consumption increased to 0.123 g/kWh for cylinders 1-3 at 100% load.

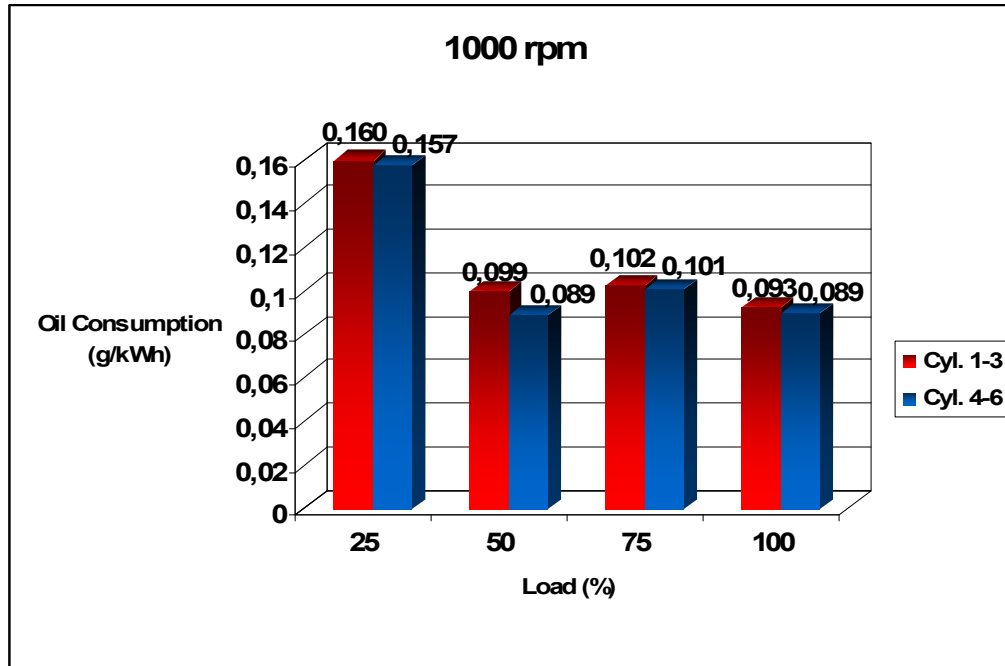


Figure 3.8 Specific Oil Consumption at 1000 rpm

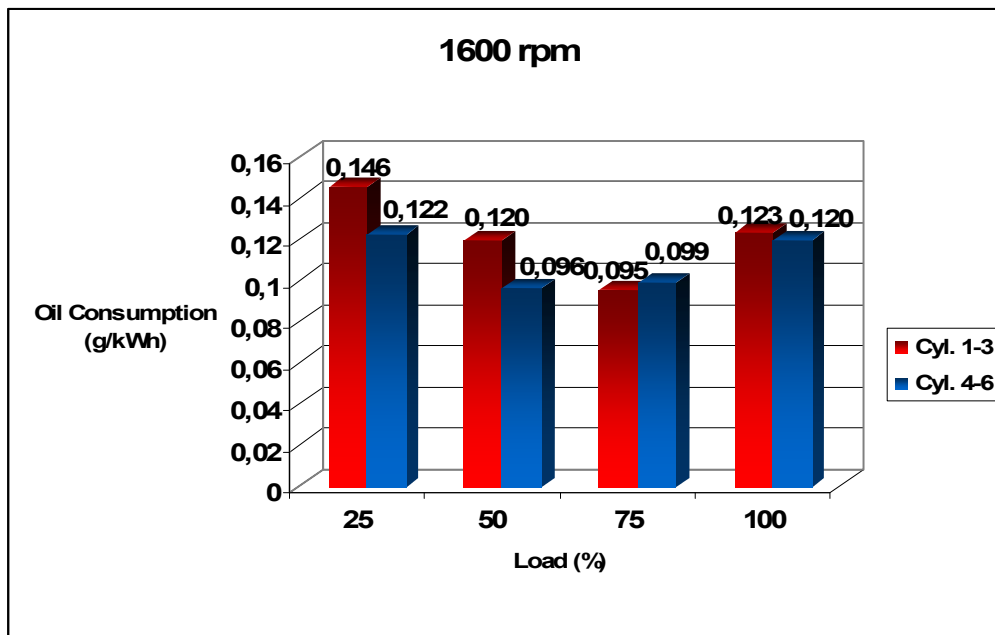


Figure 3.9 Specific Oil Consumption at 1600 rpm

Figure 3.10 demonstrates specific oil consumption results at 2200 rpm. It is assumed that power output of the engine was provided by the cylinder groups equally. As it is seen in the figure, the highest oil consumption in g/kWh for the entire test matrix was obtained at 25% load as 0.169 g/kWh.

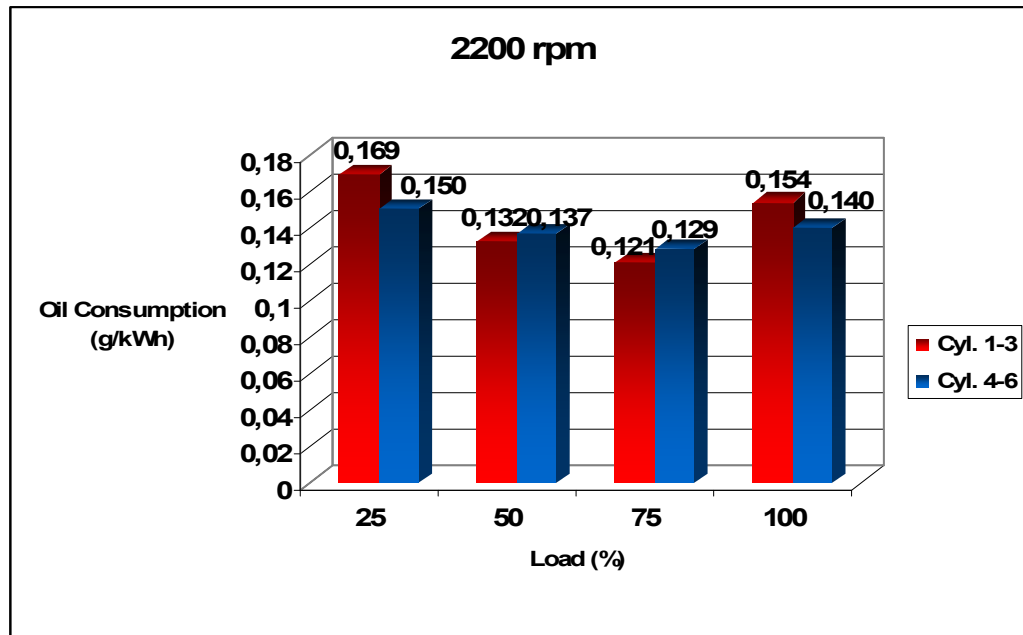


Figure 3.10 Specific Oil Consumption at 2200 rpm

In Figure 3.11, 3.12, 3.13 and 3.14 specific oil consumption results varying with engine speed at 25%, 50%, 75% and 100% load test points are presented. The results were found to be very similar to each other at 50%, 75% and 100% engine loads. On the other hand, at 50% load 2200 rpm test point and 75% load 1600 and 2200 rpm test points, the second cylinder group had higher specific oil consumption than the first cylinder group. This result can be associated with the most efficient engine operation region of specific fuel consumption. However, more investigations and experiments must be conducted in order to investigate this relation.

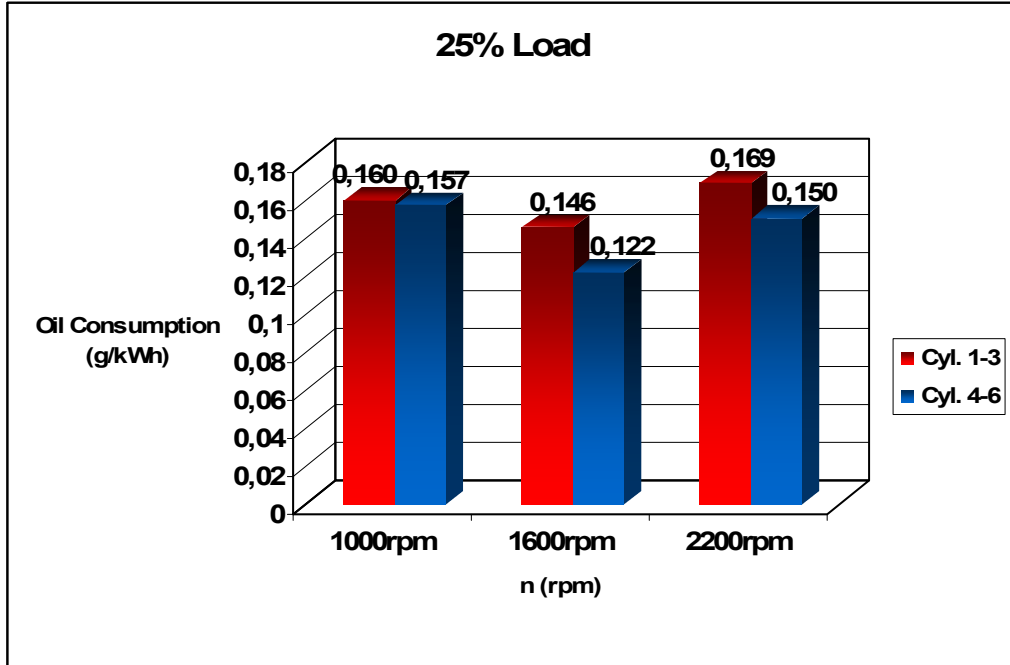


Figure 3.11 Specific Oil Consumption at 25% Load

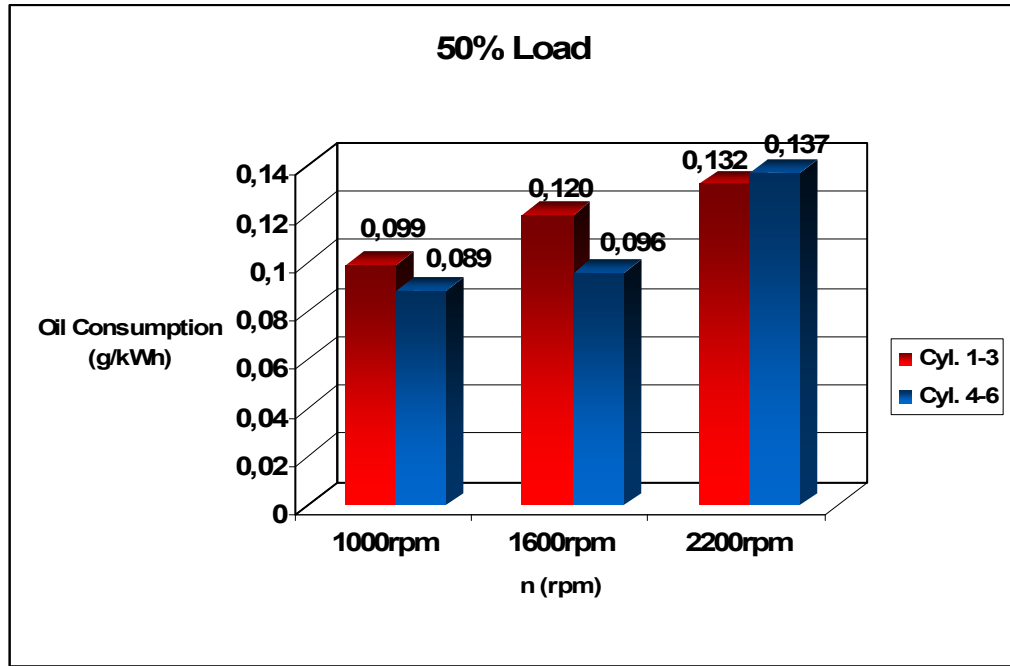


Figure 3.12 Specific Oil Consumption at 50% Load

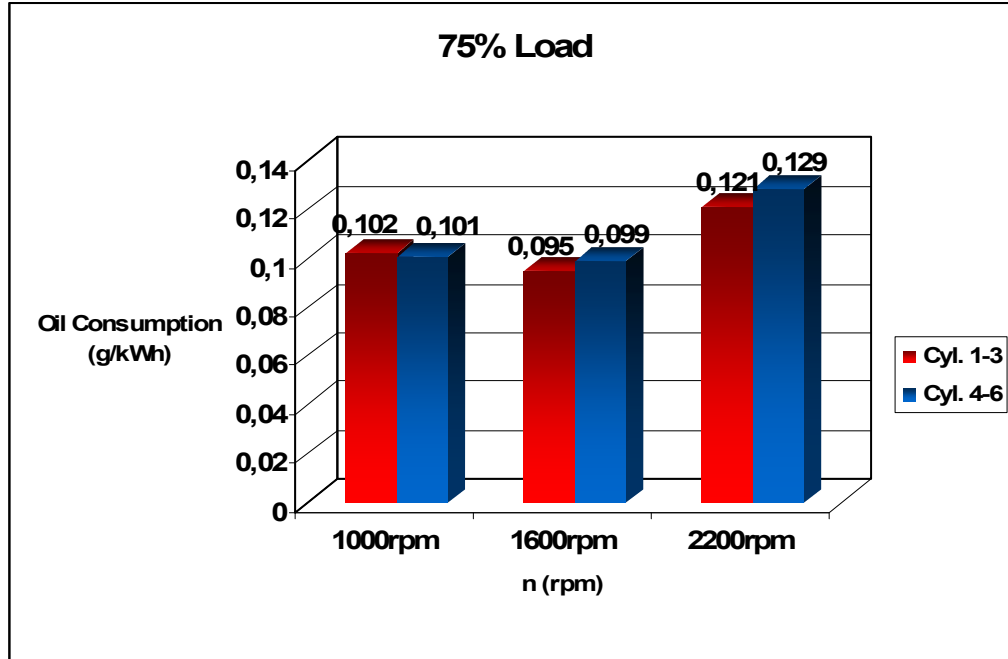


Figure 3.13 Specific Oil Consumption at 75% Load

In all results, it was observed that oil consumption records in both g/h and g/kWh increase with increasing engine speed and engine load. Higher surface roughness which was accomplished with standard plateau honing pattern increases the probability of metal-to-metal contact of surface asperities and therefore, frictional heating of the cylinder bore surface may contribute the evaporation of the lubricant as well. Additionally, rough surface may increase to surface area of the lubricant subjected to heat and accelerate the evaporation. Moreover, low surface roughness increase the tendency to develop hydrodynamic regime between piston rings and cylinder bore. Thus lower surface roughness is desirable for friction considerations in most of the engine operating conditions. However, similar results in also specific oil consumption for both separate cylinder sets demonstrate that optimization in average roughness parameters are not sufficient in order to have lower oil consumption in g/kWh. Reduced valley depth (Rvk) parameters and accordingly oil retention volume should be decreased for laser honed cylinder blocks.

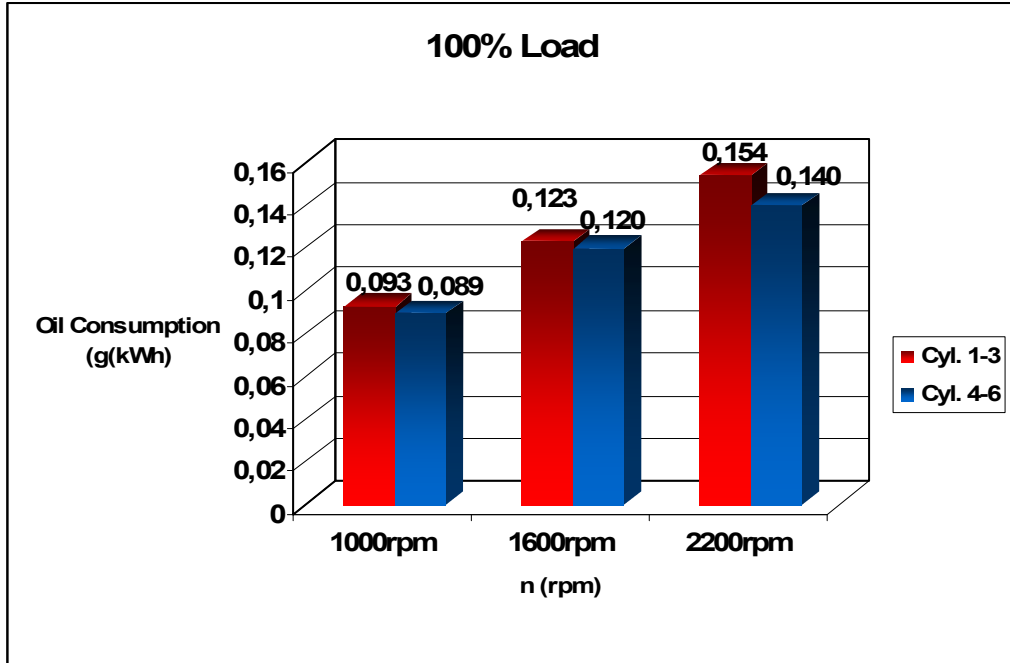


Figure 3.14 Specific Oil Consumption at 100% Load

4. CONCLUSION AND FUTURE RECOMMENDATIONS

In this study, an oil consumption method was developed in order to investigate the effects of laser surface texturing on lube oil consumption by comparing oil consumption of separate cylinder groups. This method enables the effects of power cylinder design parameters on oil consumption effectively without using any additional tracer material that may affect the lubrication characteristics. A real time oil consumption measurement test system based on collecting data from separate cylinder groups by means of a two-way valve was developed. Therefore, the possibility of obtaining considerably different results in the experiments with different engines and different operating conditions problem was eliminated. A special instrumentation which prevents the decrease in converter efficiency was designed for the system including a needle valve and a pressure sensor.

The special design of exhaust gas sampling system and measurement of real time oil consumption were accomplished in several months of time. A modified Ford ECOTORQ 9 liter heavy duty diesel engine with its first three cylinders (Cylinder 1-3) having standard plateau honing pattern and last three cylinders (Cylinders 4-6) having laser honing pattern was tested. Furthermore, test engine specification design was also unique to investigate the effects of two different configurations at upper side and lower side of the cylinder blocks. The experimental results of oil consumption (g/h) and specific oil consumption (g/kWh) were presented by means of comparative graphs based on engine power and engine speed. The highest oil consumption rate was 23.06569 g/h at 2200 rpm full load with cylinder 1-3. The results demonstrated that lube oil consumption increases with increasing speed and load. Moreover, it was observed that there is only a slight difference on lube oil consumption measurements between cylinder groups having standard plateau honing pattern and laser honing pattern. According to the experimental results and literature survey, valley material component (Mr_2) and reduced valley depth (Rvk) parameters were found to be the most effective ones on lube oil

consumption since these parameters define “Oil Retaining Volume”. Thus similar Mr_2 and Rvk parameters causing the formation of similar oil retaining volumes may be the main reason for the experimental results. Lower surface roughness is advantageous for lower oil consumption and friction. However, depending on the metrological analysis of test engine, both average roughness (Ra) and reduced valley depth (Rvk) parameters must be decreased in laser honing in order to obtain lower oil consumption measurements

In the future, the investigation of a modified engine with similar laser honing pattern but having dissimilar surface texture parameter values will be beneficial in order to provide additional acquirements on this subject. The engine blocks and cylinder liners should be carefully followed-up throughout the production period. Moreover, the adjustment of pressure in the sample line and change of the valves sequentially at each test point during the oil consumption measurements should not be done manually. In order to eliminate risks at test room and waste of time, the system must be automated. Furthermore, test system can be developed for the investigation on oil consumption contribution of each individual cylinder.

REFERENCES

- A History of Mass Spectrometry**, 2005. Retrieved February 3, 2007, from <http://masspec.scripps.edu/MSHistory/whatisms.php>
- Akalin, O., Cobanoglu, S., Toygar, A., Gul, O., Kurnaz, G., and Ergen, R. O.**, 2008. The Effects of power Cylinder design parameters on Lube Oil Consumption of A Heavy Duty Diesel Engine, *Proceedings of ASME Internal Combustion Engines Spring Technical Conference*, Chicago, Illinois, USA, April 27-30.
- Ariga, S., Sui P. And Shahed S.M.**, 1992. Instantaneous Unburned Oil Consumption Measurement in a Diesel Engine Using SO₂ Tracer Technique, *SAE Technical Paper Series*, 922196.
- AVL Internet**, 2006. Retrieved July 19, 2006, from <http://www.avl.com/wo/webobsession.servlet.go/encoded/YXBwPWJjbXMmcGFnZT12aWV3JiZub2RIaWQ9NDAwMDEzMTEAx.html>.
- Bhushan, B.**, 1999. Principles and Applications of Tribology, John Wiley, New York.
- Bhushan B.**, 2001. Modern Tribology Handbook Volume II, CRC Press, Boca Raton.
- Brizmer, V., Kligerman, Y., Etsion, I.**, 2003. A Laser Surface Textured Parallel Thrust Bearing, *Tribology Transactions*, **46**, 397-403
- Colvin, A.D., Carduner, K.R., Leong D.Y., Ames R., and Bissel H.**, 1992. An Advanced Instrument for the Real Time Measurement of Engine Oil Economy, *SAE Technical Paper Series*, 920655.
- Delvigne, T., Deconninck, B.**, 2005. A New Methodology for One Line Lubricant Consumption Measurement, *SAE Technical Paper Series*, 2005-01-2172.
- Dumitru, G., Romano, V., Weber, H. P., Haefke, H., Gerbig, Y., and Pflüger, E.**, 2000. Laser Microstructuring of Steel Surfaces for Tribological Applications. *Appl. Phys. A: Mater. Sci. Process.*, **70**, 485-487.
- Engine and A Method of Making Same**, 2007. Retrieved April 10, 2008, from <http://www.freepatentsonline.com/y2007/0101967.html>

- Etsion, I.**, 2000. Improving Tribological performance of Mechanical Seals by Laser Surface Texturing, *Proceedings of the 17th International Pump Users Symposium*, 17-22.
- Etsion, I., Halperin, G.**, 2002. A Laser Surface Textured Hydrostatic Mechanical Seal, *Tribology Transactions*, **45**, 430-434.
- Etsion, I., Halperin, G., Brizmer, V., Kligerman, Y.**, 2004. Experimental Investigation of Laser Surface Textured Parallel Thrust Bearings, *Tribology Letters*, **17**, 295-300
- Etsion, I., Kligerman, Y., and Halperin, G.**, 1999. Analytical and Experimental Investigation of Laser-Textured Mechanical Seal Faces, *Tribol. Trans.*, **42**, 511-516.
- Feldman, Y., Kligerman, Y., Etsion, I.**, 2006. A hydrostatic laser surface textured gas seal, *Tribology Letters*.
- Froelund, K.**, 1999. Real-Time Steady-State Oil Consumption Measurement on Commercial SI-Engine, *SAE Technical Paper Series*, 1999-01-3461.
- Gehring GmbH & Co. KG**, 2002. Laser Structuring-Improvement of Tribological Properties of Surfaces, Technical Brochure.
- Golloch, R., Merker, G. P., Kessen, U., and Brinkmann, S.**, 2004. Benefits of Laser-Structured cylinder Liners for International Combustion Engines in Proceedings of the 14th International Colloquium Tribology, January 13-15 Eslingen, 321-328.
- Haas, A., Geiger, U., Maaben, F.**, 1994. Oil Aeration in High Speed Combustion Engines, *SAE Technical Paper Series*, 940792.
- Hanoaka, M., Ise, A., Nagasaka, N., Osawa, H., Arakawa, Y., Obata, T.**, 1979. New Method for Measurement of Engine Oil Consumption, *SAE Technical Paper Series*, 790936
- Harris, T.**, 1991. Rolling Bearing Analysis, John Wiley & Son Ltd, New York.
- Hill, S. H.**, 2001. Cylinder Bore Finishes and Their Effect on Oil Consumption, *SAE Technical Paper Series*, 2001-01-3550.
- Hoffman, E., and Strootbant, V.** 2001. Mass Spectrometry: Principles and Applications, John Wiley & Sons, England.

- Hoppermann, A., and Kordt, M.,** 2002. Tribological Optimisation Using Laser-Structured Contact Surfaces, *O+P Oelhydraulik und Pneumatik*, **46**(4), Vereinigte Fachverlage Mainz, ISSN 0341-2660.
- Kligerman, Y., Etsion, I.,** 2001. Analysis of the Hydrodynamic Effects in a Surface Textured Circumferential Gas Seal, *Tribology Transactions*, **44**, 472-478.
- Kligerman, Y., Etsion, I., Shinkarenko, A.,** 2005. Improving Tribological Performance of Piston Rings by Partial Surface Texturing, *ASME Journal of Tribology*, **127**, 632-638.
- Kobatake S., Kawakubo, Y., Suzuki, S.,** 2003. Laplace Pressure Measurement on Laser Textured Thin-film Disk, *Tribology International*, **36**, 329-333.
- Kononenko, T. V., Garnov, S. V., Pimenov, S. M., Konov, V. I., Romano, V., Borsos, B., and Weber, H. P.,** 2000. Laser Ablation and Micropatterning of Thin TiN Coatings, *Appl. Phys. A: Mater. Sci. Process.*, **71**, 627-631.
- Kovalchenko, A., Ajayi, O., Erdemir, A., Fenske, G., Etsion, I.,** 2004. The Effect of Laser Texturing of Steel Surfaces and Speed Load Parameters on the Transition of Lubrication Regime from Boundary to Hydrodynamic, *Tribology Transactions*, **47**, 299-307.
- Laroo, C.A.,** 2002. On-Line Measurement of Sulfur Dioxide and Hydrogen Sulfide in Heavy Duty Diesel Exhaust by Chemical Ionization Mass Spectrometry, *MS Thesis*, Eastern Michigan University, Ypsilanti, MI.
- Manni, M., Carriero, M., and Roselli, A.,** 2002. A Study of Oil Consumption on a Diesel Engine with Independently Lubricated Turbocharger, *SAE Technical Paper Series*, 2002-01-2730.
- McNikel, A., and Etsion, I.,** 2004. Near-Contact Laser surface textured Dry Gas Seals, *ASME J. Tribol.* **126**(4), 788-794.
- Mourier, L., Mazuyer, D., Lubrecht, A. A., Donnet, C.,** 2006. Transient Increase of Film Thickness in Micro – Textured EHL Contacts, *Tribology International*, **39**, 1745-1756.
- Pride, S., Folkert, K., Guichelaar, P., and Etsion, I.,** 2002. Effect of Micro- Surface Texturing on Breakaway Torque and Blister Formation on carbon-Graphite Faces in a Mechanical seal, *Lubr. Eng.*, **58**, 16-21.

- Ronen, A., Etsion, I., Kligerman, Y.,** 2001. Friction Reducing Surface Texturing in Reciprocating Automotive Components, *Tribology Transactions*, **44**, 359-366.
- Ryk, G., Kligerman, Y., and Etsion, I.,** 2002. Experimental investigation of Laser Surface Texturing for Reciprocating Automotive Components, *Tribol. Trans.*, **45**(4), 444-449.
- Ryk, G., Kligerman, Y., Etsion, I., Shinkarenko, A.,** 2005. Experimental Investigation of Partial Laser Surface Texturing for Piston – Ring Friction Reduction, *Tribology Transactions*, **48**, 583-588.
- Schofield, D.M.,** 1995. Diesel Engine Instantaneous Oil Consumption Measurement By Using the Sulfur Dioxide Tracer Technique, *MS Thesis*, MIT, Cambridge, MA.
- Siripuram, R. B., Stephens, L. S.,** 2004. Effect of Deterministic Asperity Geometry on Hydrodynamic Lubrication, *ASME Journal of Tribology*, **126**, 527-534.
- Stachowiak, G., W., Batchelor, A., W.,** 2001. Engineering Tribology, Butterworth Heinemann
- Thirouard, B.,** 2001. Characterization and Modeling of the Fundamental Aspects of Oil Transport in the Piston Ring Pack of Internal Combustion Engines, *PhD Thesis*, Department of Mechanical Engineering, MIT.
- Thirouard, B. and Tian, T.,** 2003. Oil Transport in the Piston Ring Pack (Part I): Identification and Characterization of the Main Oil Transport Routes and Mechanisms, *SAE Technical Paper Series*, 2003-01-1952.
- Varenberg, M., Halperin, G., and Etsion, I.,** 2002, Different Aspects of the Role of Wear Debris in Fretting Wear, *Wear*, **252**, 902-910.
- Villinger, J., Federer, W., Resch, R., Lubich, M., Sejkora, W., Dornauer, A.,** 1993. SIMS 500 – Rapid Low Energy Secondary Ion Mass Spectrometer for In-Line Analysis of Gaseous Compounds – Technology and Applications in Automotive Emission Testing, *SAE Technical Paper Series*, 932017.
- Volchok, A., Halperin, G., and Etsion, I.,** 2002, The Effect of Surface Regular Micro-Topography on Fretting Fatigue Life, *Wear*, **253**, 509-515.

- Wang, Q. J., Zhu, D.,** 2004. Virtual Texturing: Modeling the Performance of Lubricated Contacts of Engineered Surfaces, *ASME Journal of Tribology*, **127**, 722-728.
- Wang, X., Kato, K., Adachi, K., and Aizawa, K.,** 2001. The Effect of Laser Texturing of SiC Surface on the Critical Load for the Transition of Water Lubrication Mode from Hydrodynamic to Mixed, *Tribol. Int.*, **34**(10), 703-711.
- Weng, W., and Richardson, D.E.,** 2000. Cummins Smart Oil Consumption Measuring System, *SAE Technical Paper Series*, 2000-01-0927.
- Yamada, T., Kobayashi, H., Kusama, K., Sagawa, J., Takiguchi, M. and Ishikawa, T.,** 2003. Development of a Technique to Predict Oil Consumption with Consideration for Cylinder Deformation – Prediction of Ring Oil Film Thickness and Amount of Oil Passing Across Running Surface under Cylinder Deformation, *SAE Technical Paper Series*, 2003-01-0982.
- Yilmaz, E., Tian, T., Wong, V.W., and Heywood, J.B.,** 2004. The Contribution of Different Oil Consumption Sources to Total Oil Consumption in a Spark Ignition Engine, *SAE Technical Paper Series*, 2004-01-2909.
- Yu, X. Q., He, S., and Cai, R. L.,** 2002, Frictional Characteristics of Mechanical Seals with a Laser-Textured Seal Face, *J. Mater. Process. Technol.*, **129**, 463-466.
- Zum Gahr, K.H.,** 1987. *Microstructure and Wear of Materials*, Elsevier, New York.

APPENDICES

APPENDIX A. ANALYSIS REPORT OF TEST LUBRICATING OIL

Preset Sample Data

Sample Name:	3_3 DENEYI YAG NUM.	Dilution Material:	
Description:		Sample Mass (g):	4.0000
Method:	Tql-7742	Dilution Mass (g):	0.0000
Job Number:	GOKTAN KURNAZ	Dilution Factor:	1.0000
Sample State:	Cuvette, 25 mm	Sample rotation:	No
Sample Type:	Cuvette (liquid)	Date of Receipt:	03/15/2008
Sample Status:	AAAXXX	Date of Evaluation:	03/15/2008

Results

The error is the statistical error with 1 sigma confidence interval

Z	Symbol	Element	Concentration	Abs. Error
12	Mg	Magnesium	> 0.1089 %	0.0029 %
13	Al	Aluminum	0.02653 %	0.00070 %
14	Si	Silicon	0.01082 %	0.00037 %
15	P	Phosphorus	0.1487 %	0.0006 %
16	S	Sulfur	1.172 %	0.001 %
17	Cl	Chlorine	0.01607 %	0.00008 %
19	K	Potassium	< 0.00050 %	(0.00025) %
20	Ca	Calcium	> 0.3807 %	0.0012 %
22	Ti	Titanium	< 0.00035 %	(0.0) %
23	V	Vanadium	< 0.00012 %	(0.0) %
24	Cr	Chromium	0.00038 %	0.00012 %
25	Mn	Manganese	< 0.00024 %	(0.0) %
26	Fe	Iron	0.00086 %	0.00005 %
27	Co	Cobalt	< 0.00014 %	(0.0) %
28	Ni	Nickel	< 0.00007 %	(0.0) %
29	Cu	Copper	0.00050 %	0.00004 %
30	Zn	Zinc	> 0.1297 %	0.0002 %
33	As	Arsenic	< 0.00002 %	(0.0) %
35	Br	Bromine	0.00012 %	0.00001 %
47	Ag	Silver	< 0.00026 %	(0.0) %
48	Cd	Cadmium	< 0.00029 %	(0.00021) %
50	Sn	Tin	0.00075 %	0.00025 %
51	Sb	Antimony	< 0.00063 %	(0.00039) %
52	Te	Tellurium	0.00101 %	0.00040 %
53	I	Iodine	0.00118 %	0.00072 %
56	Ba	Barium	< 0.0029 %	(0.0) %
80	Hg	Mercury	< 0.00008 %	(0.0) %
81	Tl	Thallium	0.00007 %	0.00002 %
82	Pb	Lead	0.00021 %	0.00003 %
83	Bi	Bismuth	< 0.00004 %	(0.00003) %

APPENDIX B. ANALYSIS REPORT OF TEST FUEL

Preset Sample Data

Sample Name:	3_3 DENEYI HATTAN	Dilution Material:	
Description:		Sample Mass (g):	2.0000
Method:	Sulfur	Dilution Mass (g):	0.0000
Job Number:	GOKTAN KURNAZ	Dilution Factor:	1.0000
Sample State:	Cuvette, 24 mm	Sample rotation:	No
Sample Type:	Cuvette (liquid)	Date of Receipt:	03/15/2008
Sample Status:	AXXXXX	Date of Evaluation:	

Results

The error is the statistical error with 1 sigma confidence interval

<u>Z</u>	<u>Symbol</u>	<u>Element</u>	<u>Norm.</u>	<u>No. of Impulses</u>	<u>Concentration</u>
16	S	Sulfur	10.537	7.1 mg/kg	0.3 mg/kg

APPENDIX C. MEASUREMENT RESULTS (CYLINDERS 1-3)

Table C.1 Measurement and Oil Consumption Results of Test Engine (Cylinders 1-3)

MEASUREMENTS and OIL CONSUMPTION RESULTS OF TEST ENGINE FOR CYLINDERS 1-3												
Test No.	Speed rpm	Load %	Torque Nm	Power kW	Power HP	Air Flow kg/h	Fuel Consumption kg/h	SO ₂ conc. of exhaust (ppm by volume)	Oil cons. g/h	Oil cons. g/kWh	Oil cons. g/rev	
1	2200	100	1298,826	299,589	407,324	1598,139	63,399	0,307	46,131	0,308	0,000349	
2	2200	75	1002,787	231,325	314,518	1478,871	48,805	0,205	28,074	0,243	0,000213	
3	2200	50	658,349	151,884	206,504	1353,512	33,957	0,161	20,122	0,265	0,000152	
4	2200	25	337,104	77,768	105,734	1069,021	19,793	0,134	13,126	0,338	9,94E-05	
5	1600	100	1567,417	263,030	357,622	1239,943	51,654	0,279	32,365	0,246	0,000337	
6	1600	75	1182,188	198,426	269,784	1053,847	37,425	0,194	18,885	0,190	0,000197	
7	1600	50	765,118	128,415	174,594	841,136	24,885	0,198	15,376	0,239	0,00016	
8	1600	25	388,560	65,227	88,682	633,123	13,917	0,163	9,500	0,291	9,9E-05	
9	1000	100	1123,610	118,006	160,436	465,123	23,339	0,253	10,932	0,185	0,000182	
10	1000	75	863,911	90,766	123,404	401,900	17,979	0,248	9,273	0,204	0,000155	
11	1000	50	591,295	62,146	84,493	349,583	12,585	0,192	6,178	0,199	0,000103	
12	1000	25	297,956	31,306	42,567	304,090	6,978	0,178	5,005	0,320	8,34E-05	

APPENDIX D. MEASUREMENT RESULTS (CYLINDERS 4-6)

Table D.1 Measurements and Oil Consumption Results of Test Engine (Cylinders 4-6)

MEASUREMENTS AND OIL CONSUMPTION RESULTS OF TEST ENGINE FOR CYLINDERS 4-6												
Test No.	Speed rpm	Load %	Torque Nm	Power kW	Power HP	Air Flow kg/h	Fuel Consumption kg/h	SO ₂ conc. of exhaust (ppm by volume)	Oil cons. g/h	Oil cons. g/kWh	Oil cons. g/rev	
1	2200	100	1298,826	299,522	407,233	1594,252	63,521	0,281	41,916	0,280	0,000318	
2	2200	75	1002,787	231,453	314,692	1477,944	48,815	0,217	29,798	0,257	0,000226	
3	2200	50	658,349	151,845	206,453	1349,992	33,930	0,167	20,806	0,274	0,000158	
4	2200	25	337,104	77,800	105,778	1068,478	19,790	0,120	11,703	0,301	8,87E-05	
5	1600	100	1567,417	263,026	357,617	1239,752	51,557	0,272	31,484	0,239	0,000328	
6	1600	75	1182,188	198,013	269,224	1052,238	37,328	0,201	19,588	0,198	0,000204	
7	1600	50	765,118	128,419	174,600	839,462	24,547	0,160	12,309	0,192	0,000128	
8	1600	25	388,560	65,275	88,748	633,954	13,922	0,137	7,979	0,244	8,31E-05	
9	1000	100	1123,610	118,204	160,711	466,727	23,326	0,244	10,578	0,179	0,000176	
10	1000	75	863,911	90,783	123,429	403,286	17,969	0,243	9,127	0,201	0,000152	
11	1000	50	591,295	62,146	84,499	349,332	12,531	0,172	5,513	0,177	9,19E-05	
12	1000	25	297,956	31,310	42,568	304,651	7,028	0,175	4,925	0,315	8,21E-05	

CURRICULUM VITAE

Ahu Toygar was born in Ereğli, Zonguldak, in 1983. She graduated from Kdz. Ereğli Anatolian High School in 2001 and completed her undergraduate education at the mechanical engineering faculty of Istanbul Technical University in 2005. At the same year she started her M.Sc. education at automotive division of the same faculty. She started to work as a project assistant in a cooperative industrial project between Istanbul Technical University and Ford Otosan A.Ş. in September 2007 and the project has been completed in March 2007. She is now working at Autoliv Turkey as product engineer.